AD_____

Award Number: DAMD17-98-1-8307

TITLE: Targeting Breast Cancer with Anti HER2/neu Diabodies

PRINCIPAL INVESTIGATOR: Louis M. Weiner, M.D.

CONTRACTING ORGANIZATION: Fox Chase Cancer Center
Philadelphia, Pennsylvania 19111

REPORT DATE: July 2003

TYPE OF REPORT: Final Addendum

PREPARED FOR: U.S. Army Medical Research and Materiel Command
Fort Detrick, Maryland 21702-5012

REPORT DOCUMENTATION PAGE

Form Approved
OMB No. 074-0188

1. AGENCY USE ONLY (Leave blank)	2. REPORT DATE	3. REPORT TYPE AND DATES COVERED
	July 2003	Final Addendum (22 Jun 2002 - 21 Jun 2003)

4. TITLE AND SUBTITLE
Targeting Breast Cancer with Anti HER2/neu Diabodies

5. FUNDING NUMBERS
DAMD17-98-1-8307

6. AUTHOR(S)
Louis M. Weiner, M.D.

7. PERFORMING ORGANIZATION NAME(S) AND ADDRESS(ES)
Fox Chase Cancer Center
Philadelphia, Pennsylvania 19111

E-Mail: LM_Weiner@fccc.edu

8. PERFORMING ORGANIZATION REPORT NUMBER

9. SPONSORING / MONITORING AGENCY NAME(S) AND ADDRESS(ES)
U.S. Army Medical Research and Materiel Command
Fort Detrick, Maryland 21702-5012

10. SPONSORING / MONITORING AGENCY REPORT NUMBER

11. SUPPLEMENTARY NOTES

12a. DISTRIBUTION / AVAILABILITY STATEMENT
Approved for Public Release; Distribution Unlimited

12b. DISTRIBUTION CODE

13. ABSTRACT (Maximum 200 Words)

The objective of this proposal is to develop new therapeutic reagents for breast cancer using diabody-based molecules with affinity for HER2/neu for the radioimmunotherapy (RAIT) of breast cancer. The first Technical Objective (T.O.) has focused on the optimization of the production of the selected diabody and the identification of the optimal radionuclide and labeling strategy for diabody-based RAIT. This T.O. also has involved an investigation into the impact on diabody targeting of factors likely to be encountered in a clinical setting. These include the degree of antigen density, the route (i.v. bolus or continuous infusion) and frequency of administration, the presence of disseminated disease, and the effect of antigen expression on normal tissues. Completion of these experiments has set the stage for proceeding to the clinical evaluation of diabody-based targeting of breast cancer in our second Technical Objective. Current experiments demonstrate the feasibility and efficacy of alpha particle based radioimmunotherapy wherein the radionuclide is conjugated to a chelated diabody molecule. The clinical component of this proposal will entail a Phase I radioimmunoimaging and radioimmunoguided surgery trial to elicit information on the dosimetry, specificity and tumor penetration properties of radiolabeled C6.5 diabody, and will assess the RAIT potential of this molecule.

14. Subject Terms (keywords previously assigned to proposal abstract or terms which apply to this award)
Antibodies, diabodies, single-chain Fv fragments, radioimmunotherapy, radioimmunoimaging, radioimmunoguided surgery, yttrium-90, iodine-131, astatine-211, beta particle-emitting isotopes, alpha particle-emitting isotopes, preclinical therapy studies, clinical trial

15. NUMBER OF PAGES
44

16. PRICE CODE

17. SECURITY CLASSIFICATION OF REPORT	18. SECURITY CLASSIFICATION OF THIS PAGE	19. SECURITY CLASSIFICATION OF ABSTRACT	20. LIMITATION OF ABSTRACT
Unclassified	Unclassified	Unclassified	Unlimited

Table of Contents

INTRODUCTION

The objective of this proposal was to develop new therapeutic reagents for breast cancer. We hypothesized that improved diabody-based molecules with affinity for HER2/*neu* can be engineered and will prove to be effective vehicles for the radioimmunotherapy (RAIT) of breast cancer. The first Technical Objective (T.O.) focused on the optimization of the production of the selected diabody and the identification of the optimal radionuclide and labeling strategy for diabody-based RAIT. This T.O. also involved an investigation into the impact on diabody targeting and RAIT of a variety of factors likely to be encountered in a clinical setting. These included the degree of antigen density, the route (i.v. bolus or continuous infusion) and frequency of administration, the presence of disseminated disease, and the effect of antigen expression on normal tissues. Completion of these experiments set the stage for proceeding to the clinical evaluation of diabody-based targeting of breast cancer in our second Technical Objective. The potential value of diabody-based RIT is underscored by experiments that demonstrated the feasibility and efficacy of alpha particle based radioimmunotherapy wherin the radionuclide was conjugated to a chelated diabody molecule. Despite the successful accomplishment of all preclinical elements of this project we were unable to secure additional DOD support to conduct the proof-of-concept clinical studies employing radiolabeled C6.5 diabody. We continue to endeavor to obtain such support. The clinical component would entail a Phase I radioimmunoimaging and radioimmunoguided surgery trial designed to elicit information on the dosimetry, specificity and tumor penetration properties of radiolabeled C6.5 diabody, and would assess the RAIT potential of this molecule. The successful execution of this clinical trial continues to await the identification of the support to produce clinical-grade diabody.

BODY

Technical Objectives

1. To understand the determinants of successful diabody-based tumor targeting.

2. To conduct a Phase I radioimmunoimaging and radioimmunoguided surgery (RIGS) trial of radiolabeled C6.5 diabody in women with HER-2/neu expressing breast cancers undergoing lumpectomy or mastectomy plus axillary node dissection.

3. To optimize the structure of the C6.5 diabody and create new diabody molecules targeting altenate antigens expressed in breast cancer patients.

Work Accomplished

We accomplished the important goals of defining the value of diabody-based RAIT, and showed a value in preclinical models of therapy employing beta-emitters and alpha-emitters conjugated to the C6.5 diabody. The specific impact of affinity on tumor-

targeting by diabodies was carefully examined, and we found that higher affinity did not translate into superior tumor targeting. Accordingly, the first and third technical objectives were successfully completed.

Perhaps the main accomplishment in this area was the performance of the first preclinical therapy study employing the short-lived radioisotope astatine-211 (^{211}At) conjugated to an engineered antibody-based molecule. This study (described in detail below) demonstrated the efficacy of treating solid tumors with ^{211}At-conjugated diabody molecules. The results of these studies are being prepared for submission for publication.

Despite our best efforts it proved impossible to successfully complete Technical Objective 2. It should be noted that our overarching goal has been to obtain additional support to produce GMP lots of diabody for clinical trials. In this regard we specifically applied for DOD support to achieve this goal, but did not obtain the support despite having achieved all the major preclinical milestones required to move forward into clinical development. The clinical plan was essentially identical to the plan that had been included in the current grant, and we were quite surprised and disappointed when we did not get the opportunity to move forward as we had planned. We felt the scientific review was superficial, inaccurate and uninformed and formally appealed the result, but this did not change the outcome. While we were very frustrated by this continuing impediment to translating our preclinical research into human trials, we continue to pursue multiple avenues to produce diabody that can be tested in clinical trials. We remain eager to proceed with this trial, but cannot do so unless we are able to secure support to produce GMP lots of antibody.

As noted above, we achieved all our initial specific aims with the exception of conducting a clinical trial of the ^{90}Yttrium-labeled diabody. While striving to achieve this important goal, we conducted important preclinical studies that point to new directions for diabody-based radioimmunotherapy, as listed below.

Determination of effects of antigen density on diabody targeting. Flow cytometry assays were performed using multiple cell lines (OVCAR-3, SK-BR-3, SK-OV-3, BT-474 and N87, each with varying degrees of cell surface expression of HER2/*neu*. These studies demonstrated the cell surface expression (calculated as mean fluorescence index) required for half-maximal and 100% retention, respectively, of diabody on tumor cell surfaces.

Impact of Affinity on Tumor Targeting by Diabodies. The diabody molecule is formed through the non-covalent association of two scFv molecules with short (5 amino acid) linkers between the variable-heavy and variable-light chains. The C6.5 scFv has an intrinsic binding affinity of 2.5×10^{-8} M, but in the diabody format possesses an affinity of 1.6×10^{-9} M. We used C6.5 scFv mutants with affinities for HER2/neu ranging from 10-7 M to 10-10 M but the resulting diabodies interestingly exhibited a more restricted range of affinities ($0.36 - 8 \times 10^{-9}$ M). These diabodies were radiolabeled with 125-Iodine and injected into *scid* mice bearing SK-OV-3 xenografts. We did not demonstrate affinity-dependent changes in quantitative tumor retention, tumor: blood or tumor: bone

marrow areas-under-the-curve (AUC). We concluded that the diabody format trumped other structural features as a determinant of tumor targeting.

Diabodies as Vehicles for Radioimmunodetction. Diabodies were labeled with 131-Iodine or 11-Indium and administered intravenously to *scid* mice bearing MDA-MB-361 DYT2 tumors that overexpress HER2/*neu*. The mice were imaged 24 hours later on a gamma camera. Tumor imaging was easily accomplished with 111-Indium labeled diabody, but not with 131-Iodine-labeled diabody. We found that this particular tumor line internalizes the diabody, leading to iodine catabolism and a loss of imaging sensitivity. Significant renal retention was seen with the 111-Indium radionuclide approaches, and was not significantly reduced by an unlabeled diabody preload. Since the diabody is rarely internalized by most cell lines, we expect that 131-Iodine will be suitable for imaging and therapy, and will be associated with less potential kidney toxicity than 111-Indium labeled diabody approaches. More recently we have employed 124-Iodine conjugates to examine diabody-targeted positron-emission tomography (PET) imaging and have observed exceptional imaging quality in murine preclinical models (not shown).

Unconjugated Diabody for Therapy. We conducted trials of radioimmunotherapy and used unlabeled diabody in multiple, high doses to treat nude mice bearing s.c. SK-OV-3 tumors. No anti-tumor activity was noted.

Radioimmunotherapy with 131-Iodine, 90-Yttrium and 213-Bismuth. These studies employed C6.5 diabody conjugated to 90-Yttrium and 213-Bismuth, respectively. The methods for conjugation of the diabody to these radiometals were developed and validated. We showed that 213-Bismuth was not an acceptable partner radionuclide due to its extremely rapid half-life in comparison to the carrier protein. However, 90-Yttrium proved to be a useful therapeutic conjugate, and demonstrated acceptable toxicity and significantly inhibited HER2/*neu* expressing SK-OV-3 tumor growth in treated animals at a dose of 0.3 mCi. These studies also established a model system employing nude mice for testing the toxic and therapeutic effects of a radiolabeleled diabody. Well-established palpable xenografts of the MDA-MB-361 DYT2 cell line significantly regressed, with numerous complete responders, when treated with a constant dose of diabody labeled to administer doses ranging from 0.2 – 0.3 mCi as a one-time injection.

Preclinical Therapy Studies of 211-At-C6.5 Diabody Therapy. Alpha particles have a short track length (approx. one cell in diameter). However over the course of this track length they deliver exponentially greater energy than that delivered by a beta particle. In the nucleus this high energy leads to unrepairable double stranded breaks in DNA (beta particles cause repairable single strand breaks). As such, a single alpha particle can lead to the death of a tumor cell. In general, alpha particles are emitted from radioisotopes that are too short-lived for pairing with intact antibodies. However, the 7 hour half-life of one particular alpha particle-emitting radioisotope, ^{211}At, is ideally suited for the pharmacokonetics of the C6.5 diabody. *N*-succinimidyl *N*-(4-[^{211}At]astatophenethyl) succinimate (^{211}At-SAPS) was produced by our collaborators, Drs. Brechbiel and

Waldmann of the National Cancer Institute. The compound was shipped to our lab where it was conjugated to the C6.5 diabody.

Dose escalation studies were performed with increasing doses of ^{211}AT-SAPS-C6.5 diabody specific for the HER2 tumor-associated antigen. Mice bearing established s.c. human MDA-MB-361.DYT2 breast cancer xenografts were treated with a single dose ranging from 15 to 45 μCi of ^{211}AT-SAPS-C6.5 diabody. In these studies, a clear dose response was observed with the greatest anti-tumor effect associated with the highest treatment dose (Figure 1). In the 45 μCi dose group, three of five treated animals exhibited durable complete responses, with no sign of tumor through the writing of this report (160 days post treatment) (Figure 2). In the dose ranges studied, the maximum tolerated dose has yet to be reached. All of the mice treated with ^{211}AT-SAPS-C6.5 diabody have survived the treatment with minimal observed toxicity (minor transient weight loss). As the tumors that did grow out exhibited a sudden increased rate of growth at about 35 days post treatment, the decision was made to explore the efficacy of using fractionated doses of the ^{211}AT-SAPS-C6.5 diabody at intervals of 30 days. At the time of this report, five cohorts of mice were treated with a single dose of 25 μCi of ^{211}AT-SAPS-C6.5 diabody. Four cohorts will receive a second dose two weeks from now (day 30 post the first treatment). Finally, the specificity of this therapy is being examined. The same dose range (15 to 45 μCi) that was used in the study described above and in Figure 1 has been employed in an identical study performed using the T84.66 diabody that is specific for CEA, an antigen that is not expressed in the tumor model employed. This study is still underway. The early results indicate that the control ^{211}AT-SAPS-T84.66 diabody does exhibit some anti-tumor effects, however, no complete responses have been observed (data not shown).

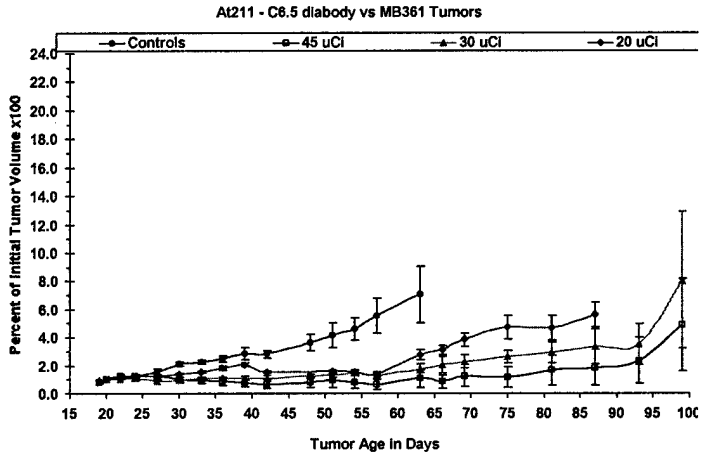

Figure 1. Mice bearing established human MDA-MB-361.DYT2 breast cancer xenografts were treated with a single dose ranging from 15 to 45 μCi of ^{211}AT-SAPS-C6.5 diabody. n = 5-7 per group. Error bars = SEM.

KEY RESEARCH ACCOMPLISHMENTS

- Determined that the unique binding format of the diabody offers significant advantages that are not explained by either size or valence of the molecule
- Demonstrated that the diabody format offers significant tumor targeting advantages that are not further enhanced by manipulating the intrinsic binding affinity of the component scFv molecules

- Demonstrated that diabodies can be used as effective therapeutic vehicles when conjugated to 131-Iodine, 90-Yttrium and 211-Astatine.

- Demonstrated that radioconjugated diabodies exhibit promise as vehicles for radioimmunodiagnosis and therapy of breast cancer that overexpresses HER2/*neu*, and that clinical development of diabodies for these purposes is warranted.

REPORTABLE OUTCOMES

Publications:

Nielsen, U.B., Adams, G.P., Weiner, L.M. and Marks, J.D.. Targeting of Bivalent Anti-ErbB2 Diabody Antibody Fragments to Tumor Cells is Independent of the Intrinsic Antibody Affinity. Cancer Res., 60:6434-6440, 2000.

Adams, G.P., Shaller, C.C., Chappel, L. Wu, C., Horak, E.M., Simmons, H.H., Litwin, S., Marks, JD., Weiner, L.M. and Brechbiel, M.W. Delivery of the alpha-emitting radioisotope Bi-213 to tumors via single-chain and diabody molecules. Nucl. Med. Biol., 27:339-46, 2000.

Powers, D.B., Amersdorfer, P., Alix-Poul, M., Refaat-Shalaby, M., Adams, G.P., Weiner, L.M. and Marks J.M. Expression of single chain Fv-Fc fusions in *Pichia Pastoris*. J. Immunol Methods, 251:123-135, 2001.

Reviews:

Adams, G.P. and Schier, R. Generating and evaluating anti-HER2/*neu* single chain Fv fragments. in *Methods in Molecular Medicine: Ovarian Cancer*. J. Bartlett (ed.) The Humana Press, Totowa, N.J. (vol. 39) 2000.

Cheng, J.D., von Mehren, M., Adams, G.P. and Weiner, L.M. Monoclonal Antibody Therapy of Cancer. Seminars in Oncology Nursing. 16(Suppl. 1):2-12, 2000.

Weiner, L.M. and Adams, G.P. New Approaches to Antibody Therapy. Oncogene. 19:6144-51, 2000

Weiner, L.M., Adams, G.P. and von Mehren, M. Monoclonal Antibodies - Therapeutic Principles. in *Cancer: Principles and Practice of Oncology, 6th Edition*. V.T. DeVita, Jr., S. Hellman and S.A. Rosenberg (eds.) pp. 495-508. J.B. Lippincott Co., Philadelphia, PA, 2001

Adams, G.P. and Weiner, L.M. Radioimmunotherapy of Solid Tumors: From Fairytale to Reality. Cancer Biotherapy & Radiopharmaceuticals. 16:9-12, 2001.

Adams, G.P. Radioimmunotherapy with Engineered Antibody Fragments. Proceedings of the 6th All Russian (International) Scientific Conference; Physical and Chemical Processes on Selection of Atoms and Molecules. Zvenigorod, Russia. 196-199. 2001.

von Mehren, M., Adams, G.P. and Weiner, L.M. Monoclonal Antibody Therapy for Cancer. Annual Review of Medicine. **54**:343-369, 2003

Abstracts and Meeting Presentations:

Nielsen, U.B., Adams, G.P., Weiner, L.M. and Marks, J.D. Targeting of bivalent anti-HER2/neu diabody antibody fragments to tumor cells is independent of intrinsic antibody affinity. Proc. Amer. Assoc. Cancer Res., 41:289, 2000.

Adams, G.P., Shaller, C.S., Horak, E.M., Simmons, H.H., Dadachova, K., Chappell, L.L., Wu, C., Marks, J.D., Brechbiel, M.W. and Weiner, L.M. Radioimmunotherapy of established solid tumor xenografts with alpha and beta emitter-conjugated antiHER2/neu single-chain Fv and diabody molecules. Presented at the Eighth Conference on Radioimmunodetection and Radioimmunotherapy of Cancer (Princeton, N.J.) Cancer Biotherapy & Radiopharmaceuticals, 15:402, 2000.

Adams, G.P. Radiolabeled and Unlabeled Engineered Antibodies for Cancer Therapy. Nuklidmötet I Umeå. Umeå, Sweden, September, 2002.

Adams, G.P. Effective Radioimmunotherapy of Solid Tumors using anti-HER2/neu Diabodies Conjugated to Alpha and Beta Particle Emitting Radioisotopes. Inaugural Russian American Scientific Conference on Radioimmunoimaging and Radioimmunotherapy. Moscow, Russia. October 2002.

Adams, G.P., Shaller, C., Garmestani, K., Tesfaye, A., Horak, E.M., Simmons, H.H., Dadachova, K., Chappell, L.L., Wu, C., Marks, J.D., Waldmann, T., Weiner, L.M., and Brechbiel M.W. Effective Radioimmunotherapy of Solid Tumors Using Anti-HER2/*neu* Diabodies Conjugated to Alpha Particle and Beta Particle Emitting Radioisotopes. Ninth Conference on Cancer Therapy with Antibodies and Immunoconjugates (Princeton, N.J.) Cancer Biotherapy & Radiopharmaceuticals, 17:481, 2002.

Adams, G.P., Shaller, C., Garmestani, K., Tesfaye, A., Waldmann, T.A. and Brechbiel, M.W. Alpha-Emitting Radioisotopes conjugated to anti-HER2/neu diabodies for the radioimmunotherapy of solid tumors. American Chemical Society 225th National Meeting, Division of Nuclear Chemistry and Technology. Abst #102, P37 Feb. 2003.

Robinson, M.K., Doss, M., Shaller, C., Manjeshwar, R.M., Gonzalez Trotter, D.E., Schneider, R., Adams, G.P., Adler, L.P. Imaging of Tumors in a Mouse Model System using a PET-based Immunodetection Methodology. Keystone Symposia - Antibody-based Therapeutics for Cancer. Banff, Alberta. Feb. 2003.

Gonzalez Trotter, D.E., Doss, M., Manjeshwar, R.M., Shaller, C., Robinson, M.K., Adams, G.P., Adler, L.P., Quantitation of Small-animal I-124 Activity Distributions Using a Dedicated Clinical PET/CT Scanner: A Phantom Study. Society of Nuclear Medicine 50th Annual Meeting, J. Nucl. Med., 44 (5):261P, 2003.

Robinson, M.K., Schneider, R., Doss, M., Narayanan, D., Shaller, C., Brogan, J., Adler, L.P., Gonzalez Trotter, D.E. and Adams, G.P. PET Imaging of Human Tumor Xenografts in a Mouse Model using Iodine-124 and Copper-64 Labeled Anti-HER2 Diabodies. 2003 Int. Conference of Academy of the Molecular Imaging. Molecular Imaging and Biology, 5:170, 2003.

Adler, L.P., Doss, M., Narayanan, D., Shaller, C., Manjeshwar, R.M., Gonzalez Trotter, D.E., Adams, G.P., Robinson, M.K. Use of a Whole Body PET/CT Scanner as a Combined Animal PET/CT Imaging Device. 2003 Int. Conference of Academy of the Molecular Imaging. Molecular Imaging and Biology, 5:133, 2003.

New Opportunities:

The most striking opportunity has arisen from our recent work with radiolabeled C6.5 diabody as a vehicle for PET imaging of tumors. As can be noted from the above abstracts, it is possible to obtain images that, when fused with structural images, should prove useful in the clinical management of women with HER2/*neu* overexpressing breast cancer.

CONCLUSION

We continue to optimize C6.5 diabody-based RAIT. ^{90}Yttrium is an excellent radionuclide partner, and ongoing work indicates that ^{211}Astatine offers an improved efficacy and toxicity profile. While we will continue our work to evaluate astatine-211, we feel that Yttrium-90 based therapy has demonstrated sufficient efficacy to justify the

initiation of a phase I clinical trial. Accordingly we will continue our attempts to secure funding for the production of GMP diabody.

REFERENCES

1. Press, O.W., Eary, J.F., Appelbaum, F.R., Martin, P.J., Badger, C.C., Nelp, W.B., Glenn, S., Butchko, G., Fisher, D., Porter, B., Matthews, D.C., Fischer, L.D. and Bernstein, I.D. Radiolabeled-antibody therapy of B-cell lymphoma with autologous bone marrow support. New England J. Med., 329:1219-1224, 1993.
2. Kaminski,, M.S., Zasady, K.R., Francis, I.R., Milik, A.W., Ross, C.W., Moon, S.D., Crawford, S.M., Burgess, J.M., Petry, N.A., Butchko, G.M., et al., Radioimmunotherapy of B-cell lymphoma with ^{131}I-anti-B1 (anti-CD20) antibody. New England J. Med., 329:459-65, 1993.
3. Jain, R.K. Transport of molecules in the tumor interstitum: a review. Cancer Res., 47:3039-3051, 1987.
4. Jain, R.K. Physiological resistance to the treatment of solid tumors. Fourth Annual IBC International Conference on Antibody Engineering, 4:87-105, 1993.
5. Juweid, M. Neumann, R. Paik, C. Perez-Bacete, M. Sato, J. vanOsdol, W and Weinstein, J.N. Micropharm-acology of monoclonal antibodies in solid tumors: direct experimental evidence for binding site barrier. Cancer Res., 52:5144-5153, 1992.
6. Fujimori, K., Covell, D.G., Fletcher, J.E. and Weinstein, J.N. Modeling analysis of the global and microscopic distribution of immunoglobulin G, F(ab')2, and Fab in tumors. Cancer Res., 49:5656-5663, 1989.
7. Colcher, D., R., Bird, R., Roselli, M., Hardman, K.D., Johnson, S., Pope, S., Dodd, S.W., Pantoliano, M.W., Milenic, D.E. and Schlom, J. In vivo tumor targeting of a recombinant single-chain antigen-binding protein. J. Natl. Cancer Inst., 82:1191-1197, 1990.
8. Milenic, D.E., Yokota, T., Filpula, D.R., Finkelman, M.A.J., Dodd, S.W., Wood, J.F., Whitlow, M., Snoy, P. and Schlom, J. Construction, binding properties, metabolism, and targeting of a single-chain Fv derived from the pancarcinoma monoclonal antibody CC49. Cancer Res., 51:6363-6371, 1991.
9. Adams, G.P., McCartney, J.E., Tai, M-S., Oppermann, H., Huston, J.S., Stafford, W.F., Bookman, M.A., Fand, I., Houston, L.L. and Weiner, L.M. Highly specific *in vivo* tumor targeting by monovalent and divalent forms of 741F8 anti-*c-erb*B-2 single-chain Fv. Cancer Res., 53:4026-4034, 1993.
10. Hollinger, P. Prospero, T. and Winter, G. "Diabodies": small bivalent and bispecific antibody fragments. Proc. Natl. Acad. Sci., USA, 90:6444-6448, 1993.
11. Zhu, Z. Zapata, G. Shalaby, R. Snedecor, B. Chen, H. and Carter, P. High level secretion of a humanized bispecific diabody from Escheria coli. BIO/TECHNOLOGY, 14:192-196, 1996.
12. Hu, S-Z. Shively, L. Raubitschek, A. Sherman, M. Williams, L. Wong, J. Shively, J. Minibody: a novel engineered anti-carcinoembryonic antigen antibody fragment(single-chain Fv-C_H3) which exhibits rapid, high-level targeting of xenografts. Cancer Res., 56:3055-3061, 1996.

13. Kim, J.A., Triozzi, P.L. and Martin, E.W. Radioimmunoguided surgery for colorectal cancer. Oncology, 7:55-60, 1993.
14. Krag, D.N., Weaver, D.L., Alex, J.C.and Fairbank, J.T. Surgical resection and radiolocalization of the sentinel lymph node in breast cancer using a gamma probe. Surg. Oncol., 2:335-340, 1993.
15. Slamon, D.J., Clark, G.M., Wong, S.G., Levin, W.J., Ullrich, A. and McGuire, W.L. Human breast cancer: correlation of relapse and survival with amplification of the HER-2/neu oncogene. Science, 235:177-182, 1987.
16. Allred, D. Clark, G. Molina, R. Tandon, A. et. al. Overexpression of HER-2/neu and its relationship with other prognostic factors change during the progression of in situ to invasive breast cancer. Hum. Pathol. 23:974-9, 1992.
17. Richman, C., DeNardo, S.J. O'Grady, L.F. and DeNardo, G.L. Radioimmunotherapy for breast cancer using escalated fractionated doses of ^{131}I-labeled chimeric L6 antibody with peripheral blood progenitor cell transfusions. Cancer Res. (Supp), 55:5916s-5920s, 1995.
18. Schrier, D.M. Stemmer, S.M. Johnson, T. et. al. High dose ^{90}Y MX-DTPA-BrE-3 and autologous hematopoietic stem cell support for treatment of advanced breast cancer: a phase I trial. Cancer Res. (Supp), 55:5921s-5924s, 1995.
19. Lewis, G. Figari, I. Fendly, B. Wong, W. Carter, P. Gorman, C.and Shepard, HM. Differential responses of human tumor cell lines to anti-p185^{HER2} monoclonal antibodies. Cancer Immun. Immnother., 37:255-263, 1993.
20. Weiner, LM. Houston, LL. Huston, JS. McCartney, J. Tai, M. Apell, G. Stafford, W. Bookman, MA. Gallo, J. and Adams, GP. Improving the tumor-selective delivery of single-chain Fv molecules. Tumor Targeting, 1:51-60, 1995.
21. Adams, GP. McCartney, J. Wolf, E. Eisenberg, J. Tai, M. Huston, J. Stafford, W. Bookman, M. Houston, LL. and Weiner, LM. Optimization of in vivo tumor targeting in scid mice with divalent forms of 741F8 anti-c-erbB-2 single-chain Fv: effects of dose escalation and repeated i.v. administration. Cancer Immun. Immunother. 40:299-306,1995.
22. Thalmann, G. Anezinis, P. Chang, S-M. Zhau, H. Kim, E. Hopwood, V. Pathak, S. von Eschenbach, A. and Chung, L.W.K. Androgen-independent cancer progression and bone marrow metastasis in the LNCaP model of human prostrate cancer. Cancer Res., 54:2577-2581, 1994.
23. Hsieh, JT. Wu, H-C. Gleave, M. von Eschenbach, A. and Chung, L.W.K. Autocrine regulation of prostrate-specific antigen gene expression in a human prostatic cancer(LNCaP) subline. Cancer Res., 53:2852-2857, 1993.
24. Garcia de Palazzo, I. Adams, G.P. Sundareshan, P. Wong, A. Testa, J. Bigner, D.D. Weiner, L.M. Expression of mutated epidermal growth factor receptor by non-small cell lung carcinomas. Cancer Res, 53:3217-3220, 1993.
25. Adams, GP. McCartney, J. Wolf, E. Eisenberg, J Huston, J Bookman, M, Moldofsky, P. Stafford, W.Houston, LL and Weiner, LM. Enhanced tumor specificity of 741F8-1 $(sFv')_2$, an anti-c-erbB-2 single-chain Fv dimer, mediated by stable radioiodine conjugation. J. Nucl. Med., 36:2276-2281, 1995.
26. Camera, L. Kinuya, S. Garmestani, K. Wu, C. Brechbiel, M. et. al. Evaluation of the serum stability and in vivo distribution of CHX-DTPA and other ligands for ^{90}Y labeling of monoclonal antibody. J. Nucl.Med. 35:882-9, 1994.

27. Behr, T.M. Sharkey, R. Juweid, M. Blumenthal, R. Dunn, R. Griffiths, G. Bair, H. Wolf, F. Becker, W and Goldenberg, DM. Reduction of the renal uptake of radiolabeled monoclonal antibody fragments by cationic amino acids and their derivatives. Cancer Res. 55:3825-3834, 1995.
28. Garcia de Palazzo, I., Klein-Szanto, A. and Weiner, L.M. Immunohistochemical detection of c-erbB-2 expression by neoplastic human tissue using monospecific and bispecific monoclonal antibodies. Intl. J. Biol. Markers, 8:233-239, 1993.
29. Weiner, L.M., Clark, J.I., Davey, M., Li, W.S., Garcia de Palazzo, I., Ring, D.B. and Alpaugh, R.K. Phase I trial of 2B1, a bispecific monoclonal antibody targeting c-erbB-2 and FcgRIII. Cancer Res., 55:4586-4593, 1995.
30. Tarburton, J. P., Halpern, S.E., Hagan, P.L., Sudora, E., Chen, A., Fridman, D.M. and Pfaff, A.E. Effect of acetylation on monoclonal antibody ZCE-025 Fab': distribution in normal and tumor-bearing mice., Journal of Biological Response Modifiers. *9:* 221-230, 1990.
31. Kunkel, T.A., Roberts, J.D. and Zakour, R.A. Rapid and efficient site-specific mutagenesis without phenotypic selection. Meth. Enzymol., 154:367-382, 1987.
32. Schier, R., McCall, A., Adams, G.P., Marshall, K.W., Merritt, H., Yim, M., Crawford, R.S., Weiner, L.M., Marks, C. and Marks, J.D. Isolation of picomolar affinity anti-c-erbB-2 single-chain Fv by molecular evolution of the complementarity determining regions in the center of the antibody binding site. J. Mol. Biol, 263:551-567, 1996.
33. Schier, R., Marks, J.D., Wolf, E., Apell, G., Wong, C., McCartney, J., Bookman, M., Huston, J., Weiner, L., and Adams, GP. In vitro and in vivo characterization of a human anti-c-erB2 single chain Fv isolated from a filamentous phage antibody library. Immunotechnology, 1:73-81, 1995.
34. Evan, G.I., Lewis, G.K., Ramsay, G., and Bishop, J.M. Isolation of monoclonal antibodies specific for human c-myc proto-oncogene product. Mol Cell Biol. 5: 3610-3616, 1985.
35. Munro, S. and Pelham, H.R.B. An Hsp-like protein in the ER: Identity with the 78kd glucose regulated protein and immunoglobulin heavy chain binding protein. Cell. 46: 291-300, 1986.
36. Breitling, S.D., Seehaus, T., Klewinghaus, I., and Little, M. A surface expression vector for antibody screening. Gene. 104: 147-153, 1991.
37. Hochuli, E., Bannwarth, W., Dobeli, H., Gentz, R., and Stuber, D. Genetic approach to facilitate purification of recombinant proteins with a novel metal chelate. Bio/Technology. 6: 1321-1325, 1988.
38. Washburn, L. Sun, T. Lee, Y. et. al. Comparison of five bifunctional chelate techniques for ^{90}Y-labeled monoclonal antibody CO17-1A. Intl. J. Rad. Appl. and Inst. - Nucl. Med. Biol., 18:313-321, 1991.
39. Loevinger, R. Budinger, T.F. and Watson, E.E. MIRD primer for absorbed dose calculations (Society of Nuclear Medicine, New York, NY), 1988.
40. Weiner, L.M., Holmes, M., Adams, G.P., LaCreta, F., et. al. A human tumor xenograft model of therapy with a bispecific monoclonal antibody targeting c-erbB-2 and CD16. Cancer Res., 53:94-100, 1993.

41. Weiner, L.M., Padavic-Shaller, K., Kitson, J., Watts, P., Krigel, R.L. and Litwin, S. Phase I evaluation of combination therapy with interleukin 2 and gamma-interferon. Cancer Res., 51:3910-3918, 1991.
42. Laub, P. and Gallo, J. NCOMP-a windows-based computer program for noncompartmental analysis of pharmacokinetic data. J. Pharm. Sci., 85:393-395, 1996.
43. Bentel, G.C., Nelson, C.E. and Noell, K.T. Treatment Planning and Dose Calculation in Radiation Oncology. pp.2-4, New York: Pergamon Press, 1989.
44. Murray, J. Macey, D. Kasi, L. Rieger, P, Cunningham, J. Bhadkamkar, V. Zhang, H Schlom, J., Rosenblum, M. and Podoloff, D. Phase II radioimmunotherapy trial with ^{131}I-CC49 in colorectal cancer. Cancer 73:1057-66, 1994.
45. Biedermann, KA. Sun, JR. Giaccia, AJ. Tosto, LM, Brown, JM. Scid mutation in mice confers hypersensitivity to ionizing radiation and a deficiency in DNA double-stand break repair. Proc. Natl. Acad. Sci. USA, 88:1394-7, 1991.
46. Hann, H-WL, Stahlhut, MW. Rubin, R. and Maddrey, WC. Antitumor effect of deferoxamine on human hepatocellular carcinoma growing in athymic nude mice. Cancer, 70:2052, 1992.134.
47. George, A. Jamar, F. Tai, M. Heelan, B. Adams, GP. et. al. Radiometal labeling of recombinant proteins by a genetically engineered minimal chelation site: Tc-99m coordination by sFv antibody fusion proteins through a C-terminal cysteinyl peptide. Proc. Natl. Acad. Sci., USA, 92:8358-8362, 1995.

LIST OF PERSONNEL PAID FROM GRANT

Louis M. Weiner, M.D., Principal Investigator
Gregory P. Adams, Ph.D., Co-Investigator
Eva Horak, M.S., Scientific Associate
Heidi Simmons, B.S., Technician

APPENDICES

Publications:

Nielsen, U.B., Adams, G.P., Weiner, L.M. and Marks, J.D.. Targeting of Bivalent Anti-ErbB2 Diabody Antibody Fragments to Tumor Cells is Independent of the Intrinsic Antibody Affinity. Cancer Res., 60:6434-6440, 2000.

Adams, G.P., Shaller, C.C., Chappel, L. Wu, C., Horak, E.M., Simmons, H.H., Litwin, S., Marks, JD., Weiner, L.M. and Brechbiel, M.W. Delivery of the alpha-emitting radioisotope Bi-213 to tumors via single-chain and diabody molecules. Nucl. Med. Biol., 27:339-46, 2000.

Powers, D.B., Amersdorfer, P., Alix-Poul, M., Refaat-Shalaby, M., Adams, G.P., Weiner, L.M. and Marks J.M. Expression of single chain Fv-Fc fusions in Pichia Pastoris. J. Immunol Methods, 251:123-135, 2001.

Abstracts:

Nielsen, U.B., Adams, G.P., Weiner, L.M. and Marks, J.D. Targeting of bivalent anti-HER2/neu diabody antibody fragments to tumor cells is independent of intrinsic antibody affinity. Proc. Amer. Assoc. Cancer Res., 41:289, 2000.

[CANCER RESEARCH 60, 6434–6440, November 15, 2000]

Targeting of Bivalent Anti-ErbB2 Diabody Antibody Fragments to Tumor Cells Is Independent of the Intrinsic Antibody Affinity[1]

Ulrik B. Nielsen, Gregory P. Adams, Louis M. Weiner, and James D. Marks[2]

Department of Anesthesiology and Pharmaceutical Chemistry, University of California, San Francisco, California 94110 [U. B. N., J. D. M.], and Department of Medical Oncology, Fox Chase Cancer Center, Philadelphia, Pennsylvania 19111 [G. P. A., L. M. W.]

ABSTRACT

In immunodeficient mice antitumor single-chain Fv (scFv) molecules penetrate tumors rapidly and have rapid serum clearance, leading to excellent tumor:normal organ ratios. However, the absolute quantity of scFv retained in the tumor is low due to rapid serum clearance and monovalent scFv binding. We previously demonstrated that the presence of an additional binding site prolongs *in vitro* and *in vivo* association of scFv-based molecules with tumor cells expressing relevant antigen. The contribution of the intrinsic affinity of each component scFv to the association between a dimeric scFv and its target antigen is largely unknown. Here, we have constructed bivalent diabody molecules from three affinity mutants of the human anti-ErbB2 (HER2/*neu*) scFv molecule C6.5 by shortening the peptide linker between the heavy (V_H) and light (V_L) chains variable domains from 15 to 5 amino acids. The shorter linker prevents intramolecular pairing of V_H and V_L, resulting in intermolecular pairing and creation of a dimeric M_r 50,000 molecule with two antigen-binding sites. The scFv used to create the diabodies span a 133-fold range of affinity for the same epitope of ErbB2 [133 nM (C6G98A), 25 nM (C6.5), and 1 nM (C6ML3–9)] and differ by only one to three amino acids. Diabody binding kinetics were determined by surface plasmon resonance on the immobilized ErbB2 extracellular domain. The association rate constants obtained for each diabody molecule were similar to that of the parental (component) scFv. However, the dissociation rate constants obtained for the bivalent diabodies were up to 15-fold slower. The magnitude of the decrease in the bivalent dissociation rate constant was inversely proportional to the monovalent interaction, ranging from only 3-fold for that of the C6ML3–9 diabody to 15-fold for the C6G98A diabody. This resulted in only a 22-fold difference in bivalent affinity, compared with a 133-fold difference in affinity for the respective scFv. Equilibrium-binding constants obtained by surface plasmon resonance correlated well with the equilibrium-binding constants determined *in vitro* on ErbB2 overexpressing cells. Biodistribution studies were performed in *scid* mice bearing established SKOV3 tumors. At 24 h, 3–37-fold more diabody was retained in tumor compared with the parental scFv monomers. This likely results from a higher apparent affinity, because of bivalent binding, and a slower serum clearance. Surprisingly, the differences in affinity between diabodies did not result in differences in quantitative tumor retention or tumor to blood ratios. In fact, the diabody constructed from the lowest affinity scFv exhibited the best tumor-targeting properties. We conclude that, above a threshold affinity, other factors regulate quantitative tumor retention. In addition, straightforward dimerization of a low-affinity scFv leads to significantly greater tumor localization than does exhaustive scFv affinity maturation.

INTRODUCTION

Mab[3]-based radioimmunotherapy of solid tumors has been hindered by the physical characteristics of IgG molecules. With a molecular weight of ~M_r 155,000, these molecules exhibit both a slow diffusion into tumors and a slow elimination from circulation. The former property leads to heterogeneous delivery into tumors, whereas the latter property results in dose-limiting myelotoxicity. Recent advances in antibody-engineering technology has led to the development of scFv molecules, composed of the variable light (V_L) and heavy (V_H) domains of an immunoglobulin molecule (1, 2). These small scFv molecules currently represent the minimal antibody-based construct capable of specifically interacting with antigen without excessive cross-reactivity. In both mice and patients their size leads to a rapid renal elimination, yielding excellent tumor:normal organ ratios and lower nonspecific background, as compared with intact IgG antibodies (3–5). In addition, the scFv penetrates more deeply into poorly vascularized regions of tumors than do the Fab', $F(ab')_2$, and intact IgG (6). However, the monovalent nature and rapid renal clearance of the scFv results in the specific retention of only small quantities in the tumors in immunodeficient mice with rarely >1%ID localized per gram of tumor at 24 h after injection (5–8). We have recently examined the tumor-targeting properties of a series of scFv mutants that vary in affinity for the same epitope of the tumor antigen ErbB2. In this model, the 24-h tumor retention of a scFv with an affinity of 133 nM (C6G98A) was indistinguishable from that achieved with an irrelevant scFv. Increasing the affinity to 25 nM (C6.5) and 1 nM (C6ML3–9) resulted in significantly greater tumor retentions of 0.8%ID/g and 1.4%ID/g, respectively (9).

We, and others, have investigated the use of larger, multivalent, scFv-based constructs to improve the degree and specificity of *in vivo* targeting of solid tumors (5, 10–13). In general, increasing the number of antigen binding sites has led to enhanced tumor retention, as compared with that achieved with monovalent scFv molecules. One of the more promising scFv-based molecules is a noncovalent dimer or diabody (14). Diabodies are constructed by shortening the scFv peptide linker from 15 aa to 5 aa. The shorter linker does not permit pairing of the V_H and V_L domains on the same polypeptide chain, forcing pairing between complementary domains of two different chains. The resulting molecule has two antigen-binding sites at opposite ends of the molecule, separated by ~65 Å (15). We have previously reported on the construction of a diabody from the C6.5 scFv, which specifically recognizes ErbB2. In tumor-bearing mice the C6.5 diabody exhibited a >7-fold increase in tumor retention without the loss of targeting specificity (16). To date, however, the relative impact of increased size, increased valance, and the affinity of the parental scFv molecules on the tumor-targeting properties of scFv dimers has yet to be elucidated.

In this study, we analyze the importance of intrinsic antibody affinity on the *in vitro* and *in vivo* targeting of ErbB2 overexpressing tumor cells using a series of diabodies constructed from the three

Received 3/27/00; accepted 9/13/00.

The costs of publication of this article were defrayed in part by the payment of page charges. This article must therefore be hereby marked *advertisement* in accordance with 18 U.S.C. Section 1734 solely to indicate this fact.

[1] Supported by National Cancer Institute Grants CA65559 and CA06927; Department of Defense Grants DAMD17-98-1-8189, DAMD17-98-1-8307, and DAMD17-94-J-4433; an appropriation from the Commonwealth of Pennsylvania, the Bernard A. and Rebecca S. Bernard Foundation, the Frank Strick Foundation, and the CaPCURE Foundation.

[2] To whom requests for reprints should be addressed, at Department of Anesthesiology and Pharmaceutical Chemistry, San Francisco General Hospital, University of California–San Francisco, Room 3C-38, 1001 Potrero Avenue, San Francisco, CA 94110. E-mail: Marksj@anesthesia.ucsf.edu.

[3] The abbreviations used are: Mab, monoclonal antibody; scFv, single-chain Fv; %ID, percentage of the injected dose; SPR, surface plasmon resonance; RU, resonance unit; ECD, extracellular domain; AUC, area under the curve; aa, amino acid.

affinity variants of the C6.5 anti-ErbB2 scFv (spanning a 133-fold range of affinity) described above. By applying SPR technology to the analysis of antigen binding, the intrinsic as well as apparent bivalent binding kinetics of the three diabodies were determined. Diabody binding to tumor cells was investigated by fluorescence cytometry using the ErbB2-positive breast cancer cell line SKOV3 to estimate equilibrium constants. Finally, biodistribution studies were performed in *scid* mice bearing established SKOV3 tumors.

MATERIALS AND METHODS

ScFv and Diabody Production. The scFv genes used for construction of diabodies were derived from the human scFv C6.5 (17, 18). Diabodies were constructed, as described previously, using a 5-aa linker between the V_H and V_L domains (16) and cloned into pUC119mycHis (17) for expression with COOH-terminal *myc* and hexahistidine epitope tags. For measurement of antibody fragment affinity on cells, the scFv and diabody genes in pUC119mycHis were amplified by PCR using the primer 5′-GCCATGGC-CGACTACAAGGCAAAGCAGGTGCAGCTGGTGCAG-3′, which adds the epitope tag DYKAK (19) recognized by the anti-FLAG M1 antibody (Sigma Chemical Co.) onto the NH_2 terminus of the scFv or diabody. The scFv and diabodies were expressed in *Escherichia coli* strain TG1. Briefly, 0.75 liter of media (2× Tryptone yeast with 100 μg/ml ampicillin and 0.1% glucose) was inoculated with an overnight culture of the appropriate plasmid in TG1, grown to an A_{600} of 0.9 and expression induced by the addition of isopropyl-β-D-thiogalactopyranoside to a final concentration of 0.5 mM. The culture was grown at 30°C for 4 h (for scFv) or overnight (for diabodies).

Cells were harvested by centrifugation (4000 × *g*, 20 min), and the pellets were resuspended on ice for 30 min in periplasmic extraction buffer [30 mM Tris, 2 mM EDTA, and 20% sucrose (pH 8.0)] containing 100 μg/ml DNase. Bacteria were pelleted by centrifugation at 5000 × *g* for 20 min, resuspended in osmotic shock buffer (5 mM $MgSO_4$), and incubated for another 20 min on ice. Bacteria were pelleted (7000 × *g*, 20 min), and supernatants from the periplasmic extraction buffer and $MgSO_4$ fractions combined and cleared by centrifugation at 10,000 *rpm* for 30 min at 4°C. The resulting solution was dialyzed in PBS. All molecules were purified by immobilized metal affinity chromatography (17), followed by size exclusion chromatography on a BioCAD SPRINT fast protein liquid chromatography system (PerSeptive Biosystems) using either a Superdex 75 (for scFv) or a Superdex 200 column (for diabodies). Protein concentrations were determined spectrophotometrically from the absorbance at A_{280} using the extinction coefficient $\epsilon = 1.4$. The C6.5 scFv-Fc fusion protein was expressed from *Pichia pastoris* and purified using protein G affinity chromatography, as described elsewhere (20).

Measurement of Binding by SPR. Association rate constants (k_{on}) were determined using SPR in a BIAcore1000 (BIAcore Inc.). Approximately 500 RU of the ErbB2 ECD were coupled to a CM5 sensor chip as described previously (17), and association rate constants were measured under continuous flow of 15 μl/min using scFv and diabody concentrations ranging from 100-1200 nM. Association rate constants were calculated from a plot of [ln(dR/dt)]/t *versus* concentration of binding sites using the BIAanalysis software (version 2.1). Apparent dissociation rate constants (k_{off}) were determined using the function BIGinjection. Different volumes [600 μl, 330 μl, 100 μl, 50 μl, and 5 μl of diabody or scFv solutions (concentration, 25 μg/ml)] were injected over the CM5 sensor chip (500 RU ECD immobilized) at a flow rate of 5 μl/min. The dissociation rate constants of all molecules were determined at >90% of maximal binding to the chip, with the exception of the C6G98A and C6.5 scFv, which were measured as close to maximal binding as possible (>50%). To determine intrinsic rate constants, diabodies were biotinylated with NHS-LC-biotin (Pierce Chemical Co.) at a biotin:diabody ratio of ~5:1 and as described by the manufacturer. Approximately 5000 RU avidin (Sigma Chemical Co.) was conjugated to a CM5 sensor chip using similar conditions as described for ErbB2 ECD (17). Biotinylated diabody was injected onto the surface to yield ~500 RU diabody bound to the surface. Saturating concentrations of ErbB2 were then injected, and dissociation rate constants were determined immediately following ErbB2 ECD dissociation. To determine their serum stability, diabodies were incubated in 90% human serum at a final concentration of 50 μg/ml for 3 days at 37°C. After diluting 10-fold in running buffer, the binding concentration was determined by SPR using immobilized ErbB2 ECD as described (18) and compared with that of the diabody stock stored at 4°C.

Cell Surface Binding Measurements. Human ovarian carcinoma SKOV3 cells (HTB 77; American Type Culture Collection) that overexpress ErbB2 were grown to 80–90% confluence in RPMI media supplemented with 10% FCS and harvested by trypsinization. Each scFv or diabody was incubated in triplicate with 1×10^5 cells in 96-well plates with V-shaped wells for 2 h at the concentrations indicated. Cell binding was performed at room temperature in PBS containing 2% FCS and 0.1% sodium azide in a total volume of 200 μl. Sodium azide was included in the incubation buffer to minimize receptor internalization. After two washes with 200 μl of PBS, bound scFv or diabody was detected by the addition of 100 μl (10 μg/ml) of FITC-labeled anti-FLAG monoclonal antibody clone M1. After incubating 30 min at room temperature, the cells were washed twice and resuspended in PBS containing 4% paraformaldehyde. Fluorescence was measured by flow cytometry in a FACSort (Becton Dickinson), and median fluorescence (F) was calculated using Cellquest software (Becton Dickinson) and the background fluorescence was subtracted. Equilibrium constants were determined as described (21), except that values were fitted to the equation $1/F = 1/F_{max} + (K_D/F_{max})(1/[scFv])$ using the software program SigmaPlot (SPSS Inc.).

Biodistribution Studies. Diabody and scFv molecules were radiolabeled with ^{125}I using the chloramine T method (^{125}I: protein ratio, 1:10), as described previously (5). The quality and immunoreactivity of the radiopharmaceuticals were evaluated by SDS-PAGE and in a live cell-binding assay as described (5). CB.17 Icr *scid* mice, 6–8 weeks of age, were obtained from the Fox Chase Cancer Center Laboratory Animal Facility. SKOV3 cells (2.5×10^6) were implanted s.c. on the abdomen of each mouse. When the tumors had achieved a size of 50–200 mg (~8 weeks), Lugol's solution was placed in their drinking water to block thyroid accumulation of radioiodine, and biodistribution studies were initiated. Twenty micrograms (100 μl) of radioiodinated diabody or scFv were administered by i.v. tail vein injection to each mouse. Cohorts of five mice that received the ^{125}I-diabodies or scFv were sacrificed at 1, 4, 8 (except C6.5db), 24, 48, and 72 h after injection. The mean and SEM of retention of each radiopharmaceutical in tissue (%ID/g) and blood (%ID/ml) were determined from decay-corrected counts, as described (5). Calculations of the estimated cumulative localization (AUC) of diabody in tumor (% h^{-1} g^{-1}) and blood (% h^{-1} ml^{-1}) were determined using the NCOMP program (22).

RESULTS

Construction, Expression, and Characterization of Recombinant scFv and Diabodies. To determine the impact of intrinsic affinity on the *in vitro* binding and *in vivo* tumor targeting of bivalent diabodies, we constructed diabodies from the scFv C6G98A, C6.5, and C6ML3–9. C6G98A and C6ML3–9 were derived from the C6.5 scFv by site-directed mutagenesis and phage display (18). The three scFv differ from each other by, at most, three amino acids, bind identical epitopes on the ErbB2 ECD and bind with K_D ranging from 1.3×10^{-7} M to 1.0×10^{-9} M (133-fold difference in K_D). Diabodies were constructed by genetically shortening the linker between the scFv from 15 to 5 aa (16). Recombinant diabodies were expressed and purified from the *E. coli* periplasm by immobilized metal affinity chromatography and size exclusion chromatography with yields of 0.5–3 mg/liter of shake flask culture. More than 90% of the purified protein was functional as determined by SPR and size exclusion chromatography in the presence of ErbB2 ECD (results not shown).

***In Vitro* Binding Kinetics of scFv and Diabodies.** The association and dissociation rate constants of the three scFv were remeasured using SPR, and the K_D was calculated as k_{off}/k_{on}. The K_D of the three scFv were comparable with values previously reported and spanned a 133-fold range of affinities (Table 1). Intrinsic diabody association and dissociation rate constants were measured to determine whether construction of diabody molecules affected the antigen binding. The association rate constant was determined by immobilizing the ECD on the sensor chip surface. The intrinsic dissociation rate constants of each diabody were determined by immobilizing biotinylated diabody

Table 1 *Comparison of intrinsic rate and equilibrium constants of scFv and diabodies*

Clone	scFv[a]			Diabody		
	k_{on} [10^5 $s^{-1}M^{-1}$]	k_{off} [10^{-3} s^{-1}]	K_D [10^{-9}M]	k_{on}[b] [10^5 $s^{-1}M^{-1}$]	k_{off}[c] [10^{-3} s^{-1}]	Intrinsic K_D[d] [10^{-9} M]
C6G98A	4.1	55	133	2.3	94	409
C6.5	4.0	10	25	2.6	8.8	34
C6ML3–9	7.6	0.76	1.0	3.9	0.78	2.0

[a] Association and dissociation rate constants for purified scFv were determined by SPR.
[b] Association rate constants (k_{on}) for purified diabodies were determined on immobilized ErbB2 ECD.
[c] Dissociation rate constants (k_{off}) of diabodies were determined by immobilizing diabody and flowing recombinant ErbB2 ECD over the surface (to avoid bivalent binding of diabody affecting the k_{off}).
[d] Equilibrium constants were calculated as $K_D = k_{off}/k_{on}$.

on an avidin-coated sensor chip. Because the recombinant ErbB2 ECD is monomeric in solution (results not shown), by immobilizing the diabody, bivalent binding is not possible and the dissociation rate constant represents that of the monovalent binding. The diabody association rate constant and the intrinsic dissociation rate constant were determined, and the intrinsic equilibrium-binding constants were calculated. These were slightly lower (2–3-fold) than the values measured for the scFv from which they were constructed, mainly as a result of decreased association rate constants (Table 1). Dissociation rate constants were similar to those of the scFv, indicating that the diabody homodimer formation does not significantly alter ligand binding to the individual binding site. The dissociation rate constant for the C6.5 scFv determined by the same approach was similar to what was determined by immobilizing ECD (results not shown).

To evaluate the contribution of the second binding site on the K_D, diabodies were analyzed for binding to immobilized ErbB2 ECD. It was hypothesized that the duration of incubation of diabody with immobilized ErbB2 ECD would affect the dissociation rate because a longer incubation would increase the likelihood of bivalent binding. To determine whether this was true, C6G98A diabody was passed over immobilized ErbB2 ECD for durations of 1–120 min. A flow rate of 5 μl/min was used for these studies because the BIGinject function for the BIAcore1000 instrument is limited by the volume of the injection loop (750 μl) and, thus, does not allow 120-min injections at faster flow rates. Although use of more rapid flow rates (15 μl/min) may minimize rebinding and yield more accurate off rates, the dissociation rate constants obtained for the scFv in this study using the 5-μl/min flow rate are comparable with our previous data using a flow rate of 15 μl/min (Ref. 18; k_{off} of C6G98A scFv = 130×10^{-3} s^{-1} at 15 μl/min *versus* 55×10^{-3} s^{-1} at 5 μl/min; k_{off} for C6.5 = 6.3×10^{-3} s^{-1} at 15 μl/min, *versus* 10×10^{-3} s^{-1} at 5 μl/min; and k_{off} for C6ML3–9 = 0.76×10^{-3} s^{-1} at both flow rates).

As expected, the rate of dissociation decreased with increasing incubation time (Fig. 1*A*). This experiment was repeated for the C6.5 and C6ML3–9 scFv and diabody, and the results were plotted as dissociation rate *versus* incubation time (Fig. 1, *B–D*). In these experiments, the apparent bivalent equilibrium constants of diabodies decreased with increased association time (Fig. 1). For C6ML3–9db, the diabody with the highest intrinsic affinity, the change in dissociation rate was only minimal over the 2-h examination period (Fig. 1*D*). However, for the C6G98Adb, which has the lowest intrinsic affinity, the dissociation rate dropped dramatically during the first 5 min of association and then stabilized (Fig. 1*B*). Similarly, for the C6.5 diabody, the dissociation rate stabilized after about 70 min of association (Fig. 1*C*). These results indicate an inverse relationship between the dissociation rate constant of a bivalent molecule and the time required to achieve bivalent binding.

In these experiments, a diabody concentration of 25 μg/ml was used because this is comparable with the predicted serum concentration in patients following the administration of therapeutic doses of Mab (23) and approximately equal to the calculated diabody dose (20 μg) used in the biodistribution studies described below. Rebinding of the diabody to the antigen matrix on the BIAcore chip will alter the measured dissociation rates. To minimize this effect, diabody dissociation rates were fitted as close to maximum binding as possible. The dissociation rate constants obtained for the C6G98A and C6.5 diabodies after 5 and 70 min of association, respectively, most likely represent the true bivalent equilibrium constants under the conditions studied.

The dissociation rate constants of the diabodies obtained after 2 h of association are reported in Table 2. The diabody apparent equilibrium constants were then calculated as k_{on}/k_{off} (after 2 h of binding; Table 2). Not surprisingly, the apparent affinity was significantly greater than the intrinsic affinity. The magnitude of the increase in affinity, however, was inversely proportional to the intrinsic affinities of the molecules (Tables 1 and 2). For the lowest affinity diabody, C6G98Adb, the increase in affinity mediated by bivalent binding was 51-fold, from 409 nM to 8 nM. Similarly, for the C6.5 diabody the affinity increased 21-fold from 34 nM to 1.6 nM as a result of bivalent binding. For the diabody with the highest affinity, C6ML3–9, the increase in apparent affinity was only 5.6-fold, from 2.0 nM to 0.36 nM. This relationship was also observed when comparing the increase in apparent affinity of the diabody to the affinity of the parental scFv

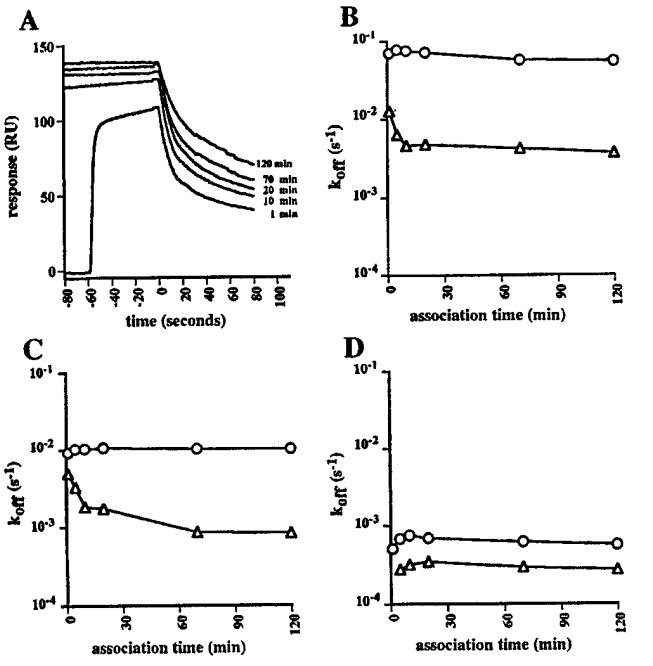

Fig. 1. Effect of association time on the dissociation rate constant (k_{off}) of scFv and diabodies as determined by SPR. *A*, C6G98A diabody (25 μg/ml) was injected at 5 μl/min for the times indicated onto ~1000 RU of ErbB2 ECD immobilized on a BIAcore CM10 chip. *B–D*, dissociation rate constants of diabody (△) or scFv (○) were determined from sensorgrams such as the one in shown in *A* and plotted as a function of time. *B*, C6G98A; *C*, C6.5; *D*, C6ML3–9.

Table 2 *Apparent diabody dissociation rate constants and equilibrium constant*

Diabody dissociation rate constants were measured on immobilized ErbB2 ECD after 2 h of association. Equilibrium constants were calculated as $K_D = k_{off}/k_{on}$.

Diabody	k_{on} [10^5 $s^{-1}M^{-1}$]	k_{off} (2-h binding) [10^{-3} s^{-1}]	Apparent K_D [10^{-9} M]	K_D scFv/K_D diabody	Intrinsic K_D diabody/ apparent K_D diabody
C6G98A	4.6	3.7	8.0	17	51
C6.5	5.2	0.84	1.6	16	21
C6ML3–9	7.8	0.28	0.36	2.8	5.6

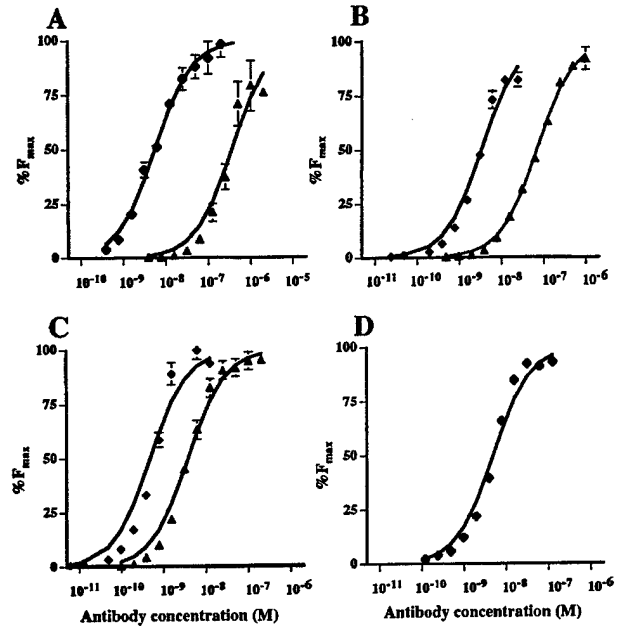

Fig. 2. Equilibrium-binding curves for scFv, diabodies, and C6.5 scFv-Fc fusion protein as determined by flow cytometry. ScFv (▲), diabodies (♦), or C6.5-fusions (◆) were incubated with SK-OV-3 cells at room temperature for 2 h, and binding was detected with anti-FLAG-FITC conjugate: *A*, C6G98A scFv and diabody; *B*, C6.5 scFv and diabody; *C*, C6ML3–9 scFv and diabody; D, bivalent C6.5 scFv-Fc fusion. Experiments were done in triplicate; *bars* represent SDs.

(17-fold, 16-fold, and 2.8-fold for C6G98A, C6.5, and C6ML3–9, respectively; Table 2). Differences between the increment in apparent K_D seen for scFv *versus* diabody are due to minor differences in the intrinsic association and dissociation rate constants that resulted from conversion of the scFv to diabody format (Table 1).

Equilibrium Constants for Binding to ErbB2-overexpressing Cancer Cells. Because the ErbB2 target antigen could be present in many orientations on the BIAcore chip, the K_D determined by SPR may not accurately reflect that measured for cell surface binding to ErbB2. Accordingly, to validate the bivalent apparent equilibrium constants determined by SPR, equilibrium constants were also determined for binding to ErbB2 expressed on the surface of SKOV3 tumor cells using fluorescence cytometry (Fig. 2). Because direct fluorescent labeling of antibody fragments is often associated with decreased affinity, diabodies were genetically tagged with an affinity-matured version of the FLAG tag (DYKAK; Ref. 19) and detected with FITC-labeled anti-FLAG M1. We determined that the affinity of the anti-FLAG antibody for the FLAG peptide tag on the diabody constructs was 2 nM (results not shown) and, thus, was similar to what has previously been published for its interaction with the synthetic peptide (19). This high-affinity interaction ensured that the secondary antibody could be used at saturating concentration. As described by Benedict *et al.* (21), these conditions are required for the measured fluorescence to be directly proportional to the amount of antibody fragment bound.

The results of these studies demonstrated that the scFv and diabody equilibrium constants on cells, as determined by flow cytometry, correlated well with the values determined by SPR (Table 3 and Fig. 2). The correlation indicates that the diabodies, despite their relatively rigid structure (15), are able to bind two ligands on the cell surface simultaneously, as observed in the more artificial SPR analysis. As with the case of equilibrium constants measured by SPR, bivalent diabodies had significantly higher apparent affinities than the parental scFv. Similarly, the increment in equilibrium constant for bivalent diabody was greatest for the lowest affinity scFv C6G98A (65-fold) and least for the highest affinity scFv (7.7-fold).

To determine whether the magnitude of the decrease in K_D for diabody binding to cells was comparable with that observed for other bivalent antibody molecules, the affinity of a C6.5-Fc fusion protein was measured (20). In this recombinant antibody molecule, the C6.5 scFv was genetically linked to the hinge, C_H2, and C_H3 domains of human IgG1. The hinge region should allow similar flexibility to the scFv-binding sites as in an IgG antibody. The scFv-Fc fusion retains the intrinsic affinity of the parental scFv (20). The affinity of the bivalent C6.5-Fc fusion for binding to cells was determined (Fig. 2*D*) and is similar to that of the C6.5 diabody (3.9 nM *versus* 3.4 nM, respectively). The results indicate that differences in binding site flexibility and size of the molecules for these two bivalent molecules does not significantly affect the affinity for binding to cell surface antigens. This result also suggests that the relationship observed between monovalent and bivalent equilibrium constants observed for diabodies is likely to hold for other bivalent antibody constructs.

Biodistribution of Diabodies in *scid* Mice Bearing ErbB2-overexpressing Tumors. The relevance of the *in vitro* observations to *in vivo* tumor targeting was determined by measuring the biodistribution of the three diabodies and the C6.5 scFv in *scid* mice bearing s.c. SKOV3 tumors overexpressing the ErbB2 antigen. The tumor, blood, and organ retention of radioiodinated scFv and diabody molecules were determined at 1, 4, 24, 48, and 72 h after i.v. administration. As expected, the larger size (50 kDa) of the diabody constructs resulted in a prolonged blood retention as compared with that seen with the smaller (25 kDa) C6.5 scFv molecule (Fig. 3, *B*, *C*, and *D* *versus* *A*). This is reflected in the 4–5-fold greater blood AUC values for the diabody molecules as compared with C6.5 scFv (Table 4). The calculated $t_{1/2}$ α for C6.5 scFv and diabody were 0.23 h and 0.67 h; the calculated $t_{1/2}$ β were 5.70 and 6.42 h, respectively. Diabodies exhibited significantly greater (2–5-fold) quantitative tumor retention at 24 h than was achieved with the highest affinity scFv studied (Fig. 3 and Table 4). This likely results from a combination of a higher apparent affinity, because of bivalent binding, and a slower serum clearance. Calculations of the cumulative residence of the radioiodinated diabodies and scFv, expressed as AUC, were determined. These were also significantly greater for diabodies compared with scFv (Table 4). Importantly, the difference in apparent affinity between diabodies did not significantly alter the quantitative tumor retention or tumor:blood ratios. In fact, the tumor AUC, tumor:blood AUC, and

Table 3 *Comparison of equilibrium constants of scFv and diabodies for binding to cells*

K_D values for binding to cells were determined by fitting the data from Fig. 2 to the Lineweaver-Burk equation.

Antibody	scFv K_D [10^{-9} M]	Diabody K_D [10^{-9} M]	K_D (scFv)/ K_D (diabody)
C6G98A	361	5.6	65
C6.5	70	3.4	18
C6ML3–9	3.8	0.49	7.7

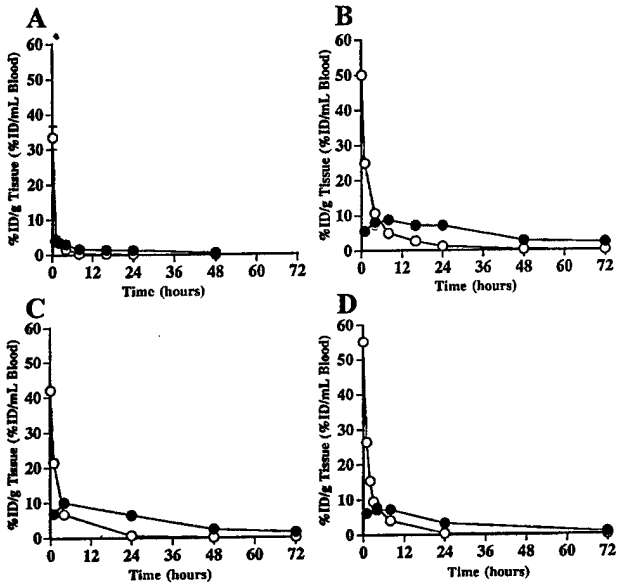

Fig. 3. The *in vivo* tumor targeting of radioiodinated scFv and diabodies. ScFv or diabody biodistribution studies were performed in SK-OV-3 tumor-bearing *scid* mice. Twenty micrograms of radioiodinated diabody or scFv were administered by i.v. tail vein injection to each mouse. Cohorts of five mice that received the ^{125}I-diabodies or scFv were sacrificed at the indicated time after injection. The plotted values represent the mean tumor (●) and blood (○) obtained from five mice per data point. *Bars* represent the SE. *A*, C6.5 scFv; *B*, C6G98A diabody; *C*, C6.5 diabody; *D*, C6ML3–9 diabody.

the 24-h tumor retention of the two lower-affinity diabodies (C6G98A and C6.5) were ~2-fold better than for the high-affinity C6ML39 diabody.

To determine whether the observed differences in AUC resulted from instability of the constructs, the diabodies were incubated in human serum for 3 days at 37°C and binding activities were compared by SPR. This study revealed that the constructs were very stable, with observed binding activities equal to 97% (C6G98A), 94% (C6.5), and 85% (C6ML3–9) of the original activity. This suggests that the observed differences in biodistribution reflect differences in the kinetic properties of the molecules, serum half-life, tumor penetration, and stability at the tumor site rather than proteolytic degradation in the circulation.

DISCUSSION

Bivalent and multivalent antibody-based molecules have recently been demonstrated to exhibit superior tumor retention properties as compared with monovalent fragments (5, 8, 11, 16, 24). Multiple approaches have been used in the construction of this class of molecules. These approaches range from direct cross-linking via a cysteine engineered onto the COOH-terminal of scFv (5) to the use of amphipathic helices to multimerize the scFv (10). However, the simplest approach takes advantage of scFv tendency to spontaneously form noncovalent dimers or diabodies. Because diabodies have molecular weights of ~M_r 50,000, they are small enough to be rapidly eliminated from the circulation via first-pass renal clearance. Because diabody size and molecular structure is similar to Fab fragments, it is expected that diabodies will readily penetrate from blood vessels into solid tumors, as reported for Fabs (6). The divalent nature of the interaction of diabodies with cell surface tumor antigen is widely recognized as being important in maintaining prolonged residence in tumors. What has been less clear is the precise relationship between the intrinsic affinity of the binding site, the increase in apparent affinity due to bivalent binding, and the impact of higher-affinity binding on *in vivo* tumor targeting.

The studies presented here were designed to examine the effect of affinity of a series of bivalent diabodies on their antigen-binding kinetics and their *in vitro* and *in vivo* tumor-targeting properties. Because all of the constructs were the same size and recognized the same epitope of ErbB2, any observed differences likely resulted solely from the differences in binding affinity. The role of valency on the impact of affinity was readily apparent when we compared the scFv and diabody constructs. The C6.5 scFv and its affinity mutants differ from each other by only one to three amino acid residues, yet differ in affinity for the same epitope of ErbB2 by 133-fold (18). However, when diabodies were constructed from the scFv, the resulting difference in affinity was reduced to only 22-fold. Most importantly, the greatest increment in affinity was observed for the diabody constructed from the lowest affinity scFv. Clearly, the kinetics of interaction is dependent on more than the straightforward additive impact of the individual affinities of the binding sites.

The equilibrium between a bivalent antibody and its antigen has often been depicted as a two-step reaction, involving free antibody and antigen as well as antibody, monovalently or bivalently complexed to its antigen. In this model, the association occurs in two steps. In the first reaction, the antibody monovalently binds to a single antigen before encountering a second antigen, after which the interaction can become bivalent. Whereas the rate of first reaction is determined by the association rate constant of the monovalent antibody arm, the second rate is dependent on external factors such as the density and fluidity of the antigen in the cell membrane (25) and the radius spanned by the antibody. In theoretical models of antibody interactions with cell surface antigen, it is often assumed that the antigen is in excess and the rate of bivalent binding solely depends on antigen diffusion (25, 26). In clinical use, however, large doses of antibody are used, potentially resulting in an excess of antibody at the binding site and the possibility of significant quantities of antigen bound monovalently.

To understand the dynamics of the binding kinetics, we studied the time dependence of bivalent binding of diabodies to ErbB2 by SPR under the conditions of high diabody concentration that might be expected in regions of tumor proximal to blood vessel. The results indicated that a large fraction of diabodies initially bind to only one antigen. Under these conditions, the bivalent dissociation rate constant decreased with increased binding time and the decrease in dissociation rate constant was inversely proportional to that of the monovalent interaction. Whereas the dissociation rate of the diabody with the lowest affinity rapidly stabilized at a 15-fold lower rate after 2 h of association, the decrease in the bivalent dissociation rate constant for the C6ML3–9 diabody was only 3-fold. One possible explanation for this result is that diabodies with lower intrinsic equilibrium constant can more rapidly achieve bivalent binding, because those bound monovalently dissociate rapidly freeing up antigen for bivalent bind-

Table 4 *Evaluation of targeting of 125I-labeled diabodies and scFv in tumor-bearing scid mice*

AUCs were calculated from the data in Fig. 3.

Antibody	Tumor AUC (% h^{-1} g^{-1})	Blood AUC (% h^{-1} ml^{-1})	Tumor: blood AUC	Calculated tumor:marrow AUC	24-h %ID/g tumor
scFv					
C6G98AscFv			ND[a]	ND	0.19
C6.5scFv	81.6	34.1	2.4:1	9.6:1	1.32
C6ML3–9scFv			ND	ND	1.42
Diabody					
C6G98Adb	433.0	178.9	2.4:1	9.6:1	7.07 ± 0.89[b]
C6.5db	405.1	132.7	3.0:1	12:1	6.48 ± 0.77
C6ML3–9db	259.1	140.5	1.8:1	7.2:1	3.18 ± 0.52

[a] ND, not determined.
[b] For the diabodies the SEs of the mean for the 24 h %ID are indicated.

ing by neighboring diabodies. Diabodies with higher intrinsic equilibrium constants dissociate more slowly from antigen and, thus, can prevent bivalent binding of neighboring diabodies. This effect has not been previously taken into account in theoretical models of bivalent binding.

The actual dynamics of the interaction between antibody and cell surface antigens in the tumor is, however, much more complex. The ability of IgG to extravasate and penetrate into tumor is severely limited by both the size of the antibody and the high hydrostatic pressure in the tumor resulting from a lack of draining lymphatics (27). This results in a very uneven distribution of the antibody, ranging from a situation of antibody excess in areas adjacent to the blood vessels to antigen excess in regions distant from the vasculature. Despite their improved tumor penetration properties, similar gradients will probably result from the administration of smaller scFv and diabody molecules (6).

In our study, the 22-fold difference in affinity (as determined by SPR) between the three diabodies did not result in greater quantitative tumor retention or tumor:blood ratio. In fact, the diabody constructed from the lowest affinity scFv (C6G98A) exhibited comparable tumor targeting to the diabody constructed from the higher-affinity C6.5 scFv and better targeting than the diabody constructed from the highest affinity C6ML3–9 scFv. Interestingly, the C6G98A scFv does not target tumor better than an irrelevant control scFv (9). We conclude that above a threshold affinity, other factors determine the quantitative tumor delivery of a bivalent antibody fragment. This is consistent with *in vivo* targeting results observed for the three C6.5-based scFv (9). This threshold affinity may be partly attributed to tumor physiology rather than simple antigen-binding kinetics. Indeed, barriers other than the antibody fragment size may exist in tumor tissue that restrict their penetration to areas distal from the blood vessels. Fujimori *et al.* (28) have postulated that high-affinity antibodies will not successfully penetrate deeply into tumors due to a binding site barrier effect, in which interaction with the first antigen encountered at the periphery of the tumor will block further diffusion of the antibody into the tumor. We have investigated the tumor penetration of the monovalent scFv used in this study. Whereas increasing the affinity improves the selective targeting of scFv to solid tumors (9) histochemical staining for scFv in the tumor xenografts supports the theory of Fujimori *et al.* (28).[4] This may explain why the C6ML3–9 diabody had significantly worse tumor-targeting properties than the other two diabodies.

In tumor-bearing immunodeficient mice, the 24-h tumor retentions of all three diabodies were superior to that of the highest affinity scFv. The differences in biodistributions of the diabodies and the scFv, thus, cannot be solely attributed to their K_D. This is apparent when comparing the tumor retention at 24 h of the C6G98A diabody to that of the higher-affinity C6ML3–9 scFv (7.1 *versus* 1.4%ID/g tumor and K_D = 5.6 nM *versus* 3.8 nM for the C6G98A diabody and C6ML3–9 scFv, respectively, for binding to cells). Clearly, the longer blood retention of the larger diabody molecules may account for some of the increased tumor retention because the diabodies would be expected to have more opportunities to perfuse the tumor and interact with target antigen. In addition, quantitative tumor localization may be affected by differences between kinetic *versus* equilibrium control of binding. The C6G98A diabody, with each binding site having a rapid dissociation rate constant, may be able to more easily dissociate from antigen and percolate through the tumor compared with a high-affinity scFv where the (single) binding site has a slower dissociation rate constant.

Differential effects of antibody fragment size, binding rates, and equilibrium constant on tumor penetration may explain the differences between our results and those of Viti *et al.* (29). In those studies, biodistributions of low-affinity (K_D = 41 nM) and high-affinity (K_D = 0.054 nM) scFv and their diabody dimers were studied in xenografted mice whose tumors expressed the neovascular antigen fibronectin. In contrast to our results, the higher-affinity scFv exhibited greater tumor retention than the diabody constructed from the lower-affinity scFv (4-fold higher %ID/g tumor at 24 h). In their model, tumor penetration is not an issue because the antigen is in the vasculature, whereas we studied an epithelial antigen where penetration will have a dramatic effect on antibody localization. A strict comparison of results between the two systems is not possible because: (*a*) Viti *et al.* (29) did not measure the apparent affinities of the diabodies; and (*b*) the "diabodies" had normal length linkers and, thus, could reequilibrate to mixtures of monomer and dimer after gel filtration and before injection into mice.

On the basis of our results, it is apparent that the construction of bivalent diabodies, even from low-affinity scFv, can lead to the generation of tumor-targeting agents that are superior to those achieved through the cumbersome processes involved in affinity maturing monovalent scFv molecules. This observation may have a significant impact on the design of future multivalent antibody-based molecules for cancer therapy.

REFERENCES

1. Huston, J. S., Levinson, D., Mudgett-Hunter, M., Tai, M. S., Novotny, J., Margolies, M. N., Ridge, R. J., Bruccoleri, R. E., Haber, E., Crea, R., and Oppermann, H. Protein engineering of antibody binding sites: recovery of specific activity in an anti-digoxin single-chain Fv analogue produced in *Escherichia coli*. Proc. Natl. Acad. Sci. USA, *85:* 5879–5883, 1988.
2. Bird, R. E., Hardman, K. D., Jacobson, J. W., Johnson, S., Kaufman, B. M., Lee, S. M., Lee, T., Pope, S. H., Riordan, G. S., and Whitlow, M. Single-chain antigen-binding proteins. Science (Washington DC), *242:* 423–426, 1988.
3. Begent, R. H., Verhaar, M. J., Chester, K. A., Casey, J. L., Green, A. J., Napier, M. P., Hope-Stone, L. D., Cushen, N., Keep, P. A., Johnson, C. J., Hawkins, R. E., Hilson, A. J., and Robson, L. Clinical evidence of efficient tumor targeting based on single-chain Fv antibody selected from a combinatorial library. Nat. Med., *2:* 979–984, 1996.
4. Colcher, D., Bird, R., Roselli, M., Hardman, K. D., Johnson, S., Pope, S., Dodd, S. W., Pantoliano, M. W., Milenic, D. E., and Schlom, J. *In vivo* tumor targeting of a recombinant single-chain antigen-binding protein. J. Natl. Cancer Inst., *82:* 1191–1197, 1990.
5. Adams, G. P., McCartney, J. E., Tai, M. S., Oppermann, H., Huston, J. S., Stafford, W. F. d., Bookman, M. A., Fand, I., Houston, L. L., and Weiner, L. M. Highly specific *in vivo* tumor targeting by monovalent and divalent forms of 741F8 anti-c-erbB-2 single-chain Fv. Cancer Res., *53:* 4026–4034, 1993.
6. Yokota, T., Milenic, D. E., Whitlow, M., and Schlom, J. Rapid tumor penetration of a single-chain Fv and comparison with other immunoglobulin forms. Cancer Res., *52:* 3402–3408, 1992.
7. Colcher, D., Pavlinkova, G., Beresford, G., Booth, B. J., Choudhury, A., and Batra, S. K. Pharmacokinetics and biodistribution of genetically-engineered antibodies. Q. J. Nucl. Med., *42:* 225–241, 1998.
8. Milenic, D. E., Yokota, T., Filpula, D. R., Finkelman, M. A., Dodd, S. W., Wood, J. F., Whitlow, M., Snoy, P., and Schlom, J. Construction, binding properties, metabolism, and tumor targeting of a single-chain Fv derived from the pancarcinoma monoclonal antibody CC49. Cancer Res., *51:* 6363–6371, 1991.
9. Adams, G. P., Schier, R., Marshall, K., Wolf, E. J., McCall, A. M., Marks, J. D., and Weiner, L. M. Increased affinity leads to improved selective tumor delivery of single-chain Fv antibodies. Cancer Res., *58:* 485–490, 1998.
10. Pack, P., and Plückthun, A. Miniantibodies: use of amphipathic helices to produce functional, flexibly linked dimeric FV fragments with high avidity in *Escherichia coli*. Biochemistry, *31:* 1579–1584, 1992.
11. Hu, S., Shively, L., Raubitschek, A., Sherman, M., Williams, L. E., Wong, J. Y., Shively, J. E., and Wu, A. M. Minibody: a novel engineered anti-carcinoembryonic antigen antibody fragment (single-chain Fv-CH3) which exhibits rapid, high-level targeting of xenografts. Cancer Res., *56:* 3055–3061, 1996.
12. Wu, A. M., Chen, W., Raubitschek, A., Williams, L. E., Neumaier, M., Fischer, R., Hu, S. Z., Odom-Maryon, T., Wong, J. Y., and Shively, J. E. Tumor localization of anti-CEA single-chain Fvs: improved targeting by non-covalent dimers. Immunotechnology, *2:* 21–36, 1996.
13. Whitlow, M., Filpula, D., Rollence, M. L., Feng, S. L., and Wood, J. F. Multivalent Fvs: characterization of single-chain Fv oligomers and preparation of a bispecific Fv. Protein Eng., *7:* 1017–1026, 1994.
14. Holliger, P., Prospero, T., and Winter, G. Diabodies: small bivalent and bispecific antibody fragments. Proc. Natl. Acad. Sci. USA, *90:* 6444–6448, 1993.

[4] G. P. Adams, R. Schier, A. M. McCall, H. Simmons, E. M. Horak, R. K. Alpaugh, J. D. Marks, and L. M. Weiner. High affinity restricts the localization and tumor penetration of single chain Fv antibody molecules, submitted for publication.

15. Perisic, O., Webb, P. A., Holliger, P., Winter, G., and Williams, R. L. Crystal structure of a diabody, a bivalent antibody fragment. Structure, *2:* 1217–1226, 1994.
16. Adams, G. P., Schier, R., McCall, A. M., Crawford, R. S., Wolf, E. J., Weiner, L. M., and Marks, J. D. Prolonged *in vivo* tumour retention of a human diabody targeting the extracellular domain of human HER2/neu. Br. J. Cancer, *77:* 1405–1412, 1998.
17. Schier, R., Marks, J. D., Wolf, E. J., Apell, G., Wong, C., McCartney, J. E., Bookman, M. A., Huston, J. S., Houston, L. L., Weiner, L. M., and Adams, G. P. *In vitro* and *in vivo* characterization of a human anti-c-erbB-2 single-chain Fv isolated from a filamentous phage antibody library. Immunotechnology, *1:* 73–81, 1995.
18. Schier, R., McCall, A., Adams, G. P., Marshall, K. W., Merritt, H., Yim, M., Crawford, R. S., Weiner, L. M., Marks, C., and Marks, J. D. Isolation of picomolar affinity anti-c-erbB-2 single-chain Fv by molecular evolution of the complementarity determining regions in the center of the antibody binding site. J. Mol. Biol., *263:* 551–567, 1996.
19. Pinilla, C., Buencamino, J., Appel, J. R., Hopp, T. P., and Houghten, R. A. Mapping the detailed specificity of a calcium-dependent monoclonal antibody through the use of soluble positional scanning combinatorial libraries: identification of potent calcium-independent antigens. Mol. Divers., *1:* 21–28, 1995.
20. Powers, D. B., Amersdorfer, P., Poul, M. A., Nielsen, U. B., Shalaby, M. R., Adams, G. P., Weiner, L. M., and Marks, J. D. Expression of single-chain Fv-Fc fusions in *Pichia pastoris*. J. Immunol. Methods, in press, 2000.
21. Benedict, C. A., MacKrell, A. J., and Anderson, W. F. Determination of the binding affinity of an anti-CD34 single-chain antibody using a novel, flow cytometry based assay. J. Immunol. Methods, *201:* 223–231, 1997.
22. Laub, P. B., and Gallo, J. M. NCOMP—a windows-based computer program for noncompartmental analysis of pharmacokinetic data. J. Pharm. Sci., *85:* 393–395, 1996.
23. DeNardo, S. J., Mirick, G. R., Kroger, L. A., O'Grady, L. F., Erickson, K. L., Yuan, A., Lamborn, K. R., Hellstrom, I., Hellstrom, K. E., and DeNardo, G. L. The biologic window for chimeric L6 radioimmunotherapy. Cancer (Phila.), *73:* 1023–1032, 1994.
24. Pavlinkova, G., Beresford, G. W., Booth, B. J., Batra, S. K., and Colcher, D. Pharmacokinetics and biodistribution of engineered single-chain antibody constructs of MAb CC49 in colon carcinoma xenografts. J. Nucl. Med., *40:* 1536–1546, 1999.
25. Kaufman, E. N., and Jain, R. K. Effect of bivalent interaction upon apparent antibody affinity: experimental confirmation of theory using fluorescence photobleaching and implications for antibody binding assays. Cancer Res., *52:* 4157–4167, 1992.
26. Crothers, D. M., and Metzger, H. The influence of polyvalency on the binding properties of antibodies. Immunochemistry, *9:* 341–357, 1972.
27. Jain, R. K. Physiological barriers to delivery of monoclonal antibodies and other macromolecules in tumors. Cancer Res., *50:* 814s–819s, 1990.
28. Fujimori, K., Covell, D. G., Fletcher, J. E., and Weinstein, J. N. Modeling analysis of the global and microscopic distribution of immunoglobulin G, F(ab')2, and Fab in tumors. Cancer Res., *49:* 5656–5663, 1989.
29. Viti, F., Tarli, L., Giovannoni, L., Zardi, L., and Neri, D. Increased binding affinity and valence of recombinant antibody fragments lead to improved targeting of tumoral angiogenesis. Cancer Res., *59:* 347–352, 1999.

Nuclear Medicine & Biology, Vol. 27, pp. 339–346, 2000

ISSN 0969-8051/00/$–see front matter
PII S0969-8051(00)00103-7

Delivery of the α-Emitting Radioisotope Bismuth-213 to Solid Tumors via Single-Chain Fv and Diabody Molecules

G. P. Adams,[1] *C. C. Shaller,*[1] *L. L. Chappell,*[2] *C. Wu,*[2] *E. M. Horak,*[1] *H. H. Simmons,*[1] *S. Litwin,*[1] *J. D. Marks,*[3] *L. M. Weiner*[1] *and M. W. Brechbiel*[2]

[1]DEPARTMENT OF MEDICAL ONCOLOGY, FOX CHASE CANCER CENTER, PHILADELPHIA, PENNSYLVANIA USA; [2]NATIONAL CANCER INSTITUTE, NATIONAL INSTITUTES OF HEALTH, BETHESDA, MARYLAND USA; AND [3]DEPARTMENT OF ANESTHESIOLOGY AND PHARMACEUTICAL CHEMISTRY, UNIVERSITY OF CALIFORNIA AT SAN FRANCISCO, SAN FRANCISCO, CALIFORNIA USA

ABSTRACT. Intravenously administered anti-tumor single-chain Fv (scFv) and diabody molecules exhibit rapid clearance kinetics and accumulation in tumors that express their cognate antigen. In an attempt to fit the rate of isotope decay to the timing of delivery and duration of tumor retention, anti-HER2/*neu* CHX-A″ DTPA-C6.5K-A scFv and diabody conjugates were labeled with the α-particle emitter ^{213}Bi ($t_{1/2}$ = 47 min). Radioimmunotherapy studies employing 0.64, 0.35, or 0.15 μCi of ^{213}Bi-labeled C6.5K-A diabody or 1.1, 0.6, or 0.3 μCi of ^{213}Bi-labeled C6.5K-A scFv were performed in nude mice bearing early, established SK-OV-3 tumors. Only the 0.3 μCi dose of ^{213}Bi-labeled C6.5K-A scFv resulted in both acceptable toxicity and a reduction in tumor growth rate. The specificity of the anti-tumor effects was determined by comparing the efficacy of treatment with 0.3 and 0.15 μCi doses of ^{213}Bi-labeled C6.5K-A scFv and ^{213}Bi-labeled NM3E2 (an irrelevant scFv) in nude mice bearing large established tumors. The 0.3 μCi dose of ^{213}Bi on both the C6.5K-A and NM3E2 scFvs resulted in similar anti-tumor effects (p = 0.46) indicating that antigen-specific targeting was not a factor. This suggests that the physical half-life of ^{213}Bi may be too brief to be effectively paired with systemically-administered diabody or scFv molecules. NUCL MED BIOL 27;4: 339–346, 2000.

KEY WORDS. α Particles, Single-chain Fv, Diabody, Radioimmunotherapy, Solid tumors

INTRODUCTION

The field of radioimmunotherapy (RAIT) has been recently buoyed by reports of successes in the treatment of hematologic malignancies with ^{131}I-labeled (17, 29) and ^{90}Y-labeled (19) monoclonal antibodies (MAb). Although sporadic reports of success exist for RAIT of solid tumors (5), these rates are far below those achieved in diffuse malignancies. This is largely due to the physiology of solid tumors. Unlike normal tissues, tumors lack draining lymphatics and consistently outgrow their blood supply (15, 16). As a result, high hydrostatic pressures develop inside the tumor, which in turn limit the diffusion of large macromolecules (e.g., intact immunoglobulin G [IgG]) into the tumor microenvironment.

In an attempt to circumvent these impediments, application of smaller engineered antibody-based proteins has been developed. The 25-kDa single-chain Fv (scFv) and the 50-kDa diabody are two such molecules. The scFv is composed of the variable light and variable heavy chains of an IgG molecule joined by a 15 amino acid spacer that holds the two chains together and allows them to form a single binding pocket (14). In contrast, the diabody is a scFv dimer formed by shortening the spacer between the light and heavy chains from 15 to 5 amino acids, thereby preventing the chains from a single molecule from associating to form a binding pocket (13). Because the light and heavy chains have a high affinity for each other, the light chain from one molecule associates with the heavy chain of a second (and vice versa), leading to the production of a noncovalent dimer.

Small engineered scFv and diabody molecules are rapidly cleared from the circulation of immunodeficent mice, leading to highly specific tumor retention of minimal quantities of radionuclide in the terminal phases of their distribution (2, 3, 8, 24, 35, 36). However, their small sizes also allow for a rapid delivery to tumor and mediate effective tumor penetration. Because these final two properties are highly desirable in the selection of effective agents for the RAIT of solid tumors, the challenge remains to pair these molecules with isotopes that are well matched to rapid transit to tumor and relatively transient tumor retention. In mice, the majority of the tumor residence occurs within the first 12 h after injection for the scFv and within the first 24 h after injection for the diabody. Because the classical RAIT isotope ^{131}I has a half-life of 192 h, ^{131}I conjugated to a scFv or diabody will likely undergo most of its disintegrations long after the radioimmunoconjugate has cleared from the tumor and has been eliminated from the host. Similarly, the shorter-lived isotope ^{90}Y ($t_{1/2}$ = 64 h) may still have too long a physical half-life to be effective in this setting. In a study describing the potential of anti-CEA diabodies to serve as vehicles for the delivery of short-lived isotopes for RAID, Wu *et al.* (36) reported optimal planar imaging of human tumor xenografts in athymic mice at 6 h and the ability to detect the tumors as early as 2 h after administration of ^{123}I-labeled diabody (physical $t_{1/2}$ = 13.2 h). In the same study, it was calculated that the optimal time for positron emission tomography (PET) imaging with ^{18}F-labeled

Supported by National Cancer Institute Grant CA65559, Department of Defense Grant DAMD17-98-1-8307, the Bernard A. and Rebecca S. Bernard Foundation, the Frank Strick Foundation, and an appropriation from the Commonwealth of Pennsylvania.

Address correspondence to: G. P. Adams, Ph.D., Department of Medical Oncology, Fox Chase Cancer Center, 7701 Burholme Ave., Philadelphia, PA 19111; e-mail: gp_adams@fccc.edu.

Received 1 March 2000.
Accepted 21 March 2000.

diabody (physical $t_{1/2}$ = 110 min) would occur 1.4 h after administration.

The use of the α emitters, namely ^{212}Bi, ^{213}Bi, and ^{211}At, have recently attracted attention for their potential use in RAIT. In particular, ^{213}Bi ($t_{1/2}$ = 47 min) has been proposed as a viable candidate due to a combination of availability and the lack of a requirement for specialized production and labeling facilities. In addition, it has been proposed that successful RAIT will result from the matching of half-lives of the isotope and the delivery vector (10, 11). Finally, the track length of α particles is significantly shorter than that of β particles (22). Therefore, when employed for RAIT, the cytotoxicity should be more focused at tumor sites with less potential for collateral damage of normal tissue.

In the current study we have conjugated the anti-HER2/*neu* C6.5K-A scFv and diabody molecules to CHX-A″, a single enantiomer of 2-(*p*-isothiocyanatobenzyl)-cyclohexyl-diethylenetriaminepentaacetic acid (CHX-DTPA), which is a recently developed backbone-substituted derivative of DTPA (38). Using these radioimmunoconjugates, we have begun to determine the conditions that may lead to the most favorable pairing of isotopes with the new generation of engineered antibody fragments.

MATERIALS AND METHODS

The C6.5K-A scFv (C6.5K100gA) and diabody molecules differ from the native C6.5 sequence by a single amino acid substitution in the heavy chain CDR3 (30, 31). This format was employed because the original C6.5 molecule has a lysine in the heavy chain CDR3 that prohibits use of chelate conjugation strategies that target amino groups. The C6.5K-A and C6.5 scFv molecules both have similar affinities (31) and biodistributions when labeled with ^{125}I by the chloramine T method (data not shown). Both molecules were produced by periplasmic expression from *Escherichia coli* in shake flasks and purified by immobilized metal affinity chromatography (IMAC) and subsequent size exclusion chromatography as previously described (30, 31).

Conjugation

The bifunctional chelating agent CHX-A″ DTPA (38) was conjugated to the C6.5K-A scFv, the C6.5K-A diabody, and an irrelevant negative control scFv NM3E2 (specific for CD16) as previously described (25). The final antibody concentration was measured spectrophotomerically using an extinction coefficient of 1.4 mL/mg/cm for the scFv and diabody molecules, and the chelate to protein ratio was determined as described in the literature (28).

^{213}Bi-Labeling

^{213}Bi was selectively eluted from a generator that had been prepared with 20 μCi ^{225}actinium chloride ($^{225}AcCl_3$; Oak Ridge Natl. Laboratories, Oak Ridge, TN USA) as described in the literature (37). Briefly, two syringes containing 25 mL of metal-free water and one syringe containing 11 mL ultrapure 1.0 M HCl were placed on a syringe pump set at the rate of 1 mL/min. Tubing from all three syringes combined in an acrylic mixing chamber containing a magnetic stir bar. The effluent from the mixing chamber was then introduced into the generator, displacing the ^{213}Bi into an AG 50WX4 cation resin column. ^{213}Bi was eluted from the cation resin with 0.8 mL of 0.1 M HI. The eluted ^{213}Bi was neutralized to pH 5.0 by the addition of 40 μL of 5.0 M NaOAc and the radioisotope was incubated with 300–400 μg of CHX-A″ conjugated scFv or diabody for 10 min at room temperature. Ten microliters of 0.1 M ethylene diamine tetraacetic acid (EDTA) were added to chelate any unincorporated ^{213}Bi and the labeled proteins were purified by the centrifuged Sephadex G50-80 column method (23). The specific activity of the ^{213}Bi radiopharmaceuticals was determined using a dose calibrator (Capintech Model CRC-35R, Capintech Inc., Ramsey, NJ USA) set at the National Institute of Standards and Technology dictated setting of 38. The quality of the labeled scFv and diabody molecules was assessed by ITLC and in live cell binding assays (1). In the ITLC assays, 1 μL from each reaction mixture and final product was applied to silica ITLC strips (Biodex Medical Systems, Shirley, NY USA) and allowed to migrate using normal saline as a mobile phase. The strips were cut at the midpoint and the top and bottom halves were counted in a gamma well counter (Gamma4000, Beckman, Irvine, CA USA). The immunoreactivities of the radiopharmaceuticals were determined in a live cell binding assay (1). Briefly, 10 ng of labeled scFv or diabody in 100 μL phosphate-buffered saline (PBS) was added in triplicate into 15 mL polypropylene centrifuge tubes containing 5 × 10^6 SK-OV-3 human ovarian carcinoma cells (HTB 77; ATCC), which overexpress the HER2/*neu* antigen. The cells were allowed to incubate for 30 min at room temperature. Two milliliters of PBS were added to each tube and they were centrifuged for 5 min at 500 × g. Supernatants were separated from the cell pellets, both were transferred to 12 × 75 counting tubes and the percentage of radioactivity associated with the cell pellet was determined by counting in a gamma-counter.

Therapy Studies

SK-OV-3 cells were implanted subcutaneously in the abdomens of 8-week-old male athymic nude mice (Taconic Labs, Germantown, NY USA). The first therapy study was performed at 10 days following the implantation of 5 × 10^6 cells (mean tumor size = 68 ± 5 mm^3). To reduce the nontargeted renal and reticuloendothelial retention of the ^{213}Bi, each mouse was given 100 mg of L-lysine (Sigma Chemical Co., Cat. #L-6027, St. Louis, MO USA) in 250 μL of normal saline by intraperitoneal injection 2 h prior to initiating the therapy study. Cohorts of five mice were treated with ^{213}Bi-labeled CHX-A″-C6.5K-A diabody, ^{213}Bi-labeled CHX-A″-C6.5K-A scFv, or unlabeled C6.5K-A diabody or scFv. The mice treated with ^{213}Bi-labeled CHX-A″-C6.5K-A diabody received 640, 400, or 150 μCi (72, 48, and 16 μg, respectively). Mice treated with ^{213}Bi-labeled CHX-A″-C6.5K-A scFv received 1,100, 600, or 300 μCi (300, 196, and 102 μg, respectively). The tumors were measured with calipers and body weights were obtained two to three times weekly. The mice were also observed for signs of toxicity. Tumor volumes were determined using the ellipsoidal formula: length (mm) × width (mm) × height (mm) × 0.52 (derived from π/6) (12). The study was terminated when tumor volumes exceeded 10% of the animal's body weight.

A second therapy study was performed to determine if the tumor growth inhibition observed with ^{213}Bi-labeled CHX-A″-C6.5K-A scFv treatment in the initial study was specific in nature. In this case, mice bearing established SK-OV-3 tumors (mean tumor size = 16.6 ± 8.1 mm^3) were employed 30 days after the subcutaneous implantation of 2.5 × 10^6 cells. Cohorts of mice were treated with a single intravenous injection of ^{213}Bi-labeled CHX-A″ conjugated to either the C6.5K-A scFv (10 mice per treatment group) or the NM3E2 scFv (5–6 mice per treatment group), which is specific for CD16 antigen that is not expressed in the mouse. Treatment doses were 300 μCi (166–340 μg) or 150 μCi (83–110 μg) of ^{213}Bi-

labeled CHX-A″ conjugated to either scFv. Control mice were treated with 80 μg of unconjugated (cold) C6.5K-A scFv. Tumor measurements and animal weights were acquired every 3–4 days and tumor volumes were calculated as described above. The study was terminated when the mice became moribund or when their tumor volumes exceeded 10% of the animal's weight. The significance of the difference in growth rates of the tumors in the treatment and control groups was determined using Wilcoxon one-sided tests.

RESULTS

Antibodies

The C6.5K-A scFv and C6.5K-A diabody molecules employed in the first therapy study were determined to have an average of 0.55 and 0.48 CHX-A″ ligands associated per antibody molecule, respectively. The C6.5K-A scFv and NM3E2 scFv molecules employed in the second therapy study had 1.1 and 0.8 CHX-A″ ligands associated per antibody molecule, respectively. In the ITLC assays of the radiopharmaceuticals, it was determined that 97% (C6.5K-A diabody), 96% (C6.5K-A scFv, first study), 98% (C6.5K-A scFv, second study), and 97% (NM3E2 scFv) of the activity did not migrate and thus was protein associated. The average immunoreactivities were well within the customary range for each anti-HER2/*neu* molecule, with values of 57% and 64%, respectively, for the C6.5K-A scFv and diabody molecules and less than 2% for the NM3E2 scFv negative control.

Therapy Studies

The initial therapy study was performed to determine the maximum tolerated dose (MTD) of ^{213}Bi-labeled CHX-A″-C6.5K-A scFv and diabody molecules and to acquire preliminary evidence of the efficacy of utilizing these conjugated α emitters for the treatment of solid tumors. To assess the MTD, weight measurements of the treated mice were acquired two to three times per week and they were observed for outward signs of toxicity. The mice treated with the 640 μCi and 400 μCi doses of ^{213}Bi-labeled CHX-A″-C6.5K-A diabody exhibited marked decreases in body weight (29 ± 7%) within 6 days following receipt of treatment. By day 7, all of the 640 μCi group and two of the five mice in the 400 μCi group had died (Fig. 1B). Although the mice that received the 150 μCi dose of ^{213}Bi-labeled CHX-A″-C6.5K-A diabody did not exhibit a similar weight loss, the dose was still lethal in two of the five treated animals. Similar toxicities were observed with the ^{213}Bi-labeled CHX-A″-C6.5K-A scFv. However, its faster equilibration and elimination phases in circulation were associated with a higher MTD for ^{213}Bi. This was demonstrated by the survival of all of the animals that received the 300 μCi dose (Fig. 1A). However, the dose was still toxic, as evidenced by an average weight loss of 10% by the tenth day after the treatment. As above with the diabody, the greatest toxicity was observed in the two higher dose groups. Both 1,100 μCi and 600 μCi doses of ^{213}Bi-labeled CHX-A″-C6.5K-A scFv were completely lethal (Fig. 1A).

The therapeutic efficacies of treatment at the best-tolerated doses in the first study are displayed in Figure 2. In this experiment, the 300 μCi of ^{213}Bi-labeled CHX-A″-conjugated C6.5K-A scFv led to an approximately 2-week delay in the doubling time of the early subcutaneous SK-OV-3 tumors compared with that observed in the untreated control group (34 days versus 21 days, respectively; Fig. 2A). In contrast, a 150 μCi dose of ^{213}Bi-labeled CHX-A″-C6.5K-A diabody did not significantly alter the tumor growth rate from that observed in the untreated mice (Fig. 2B).

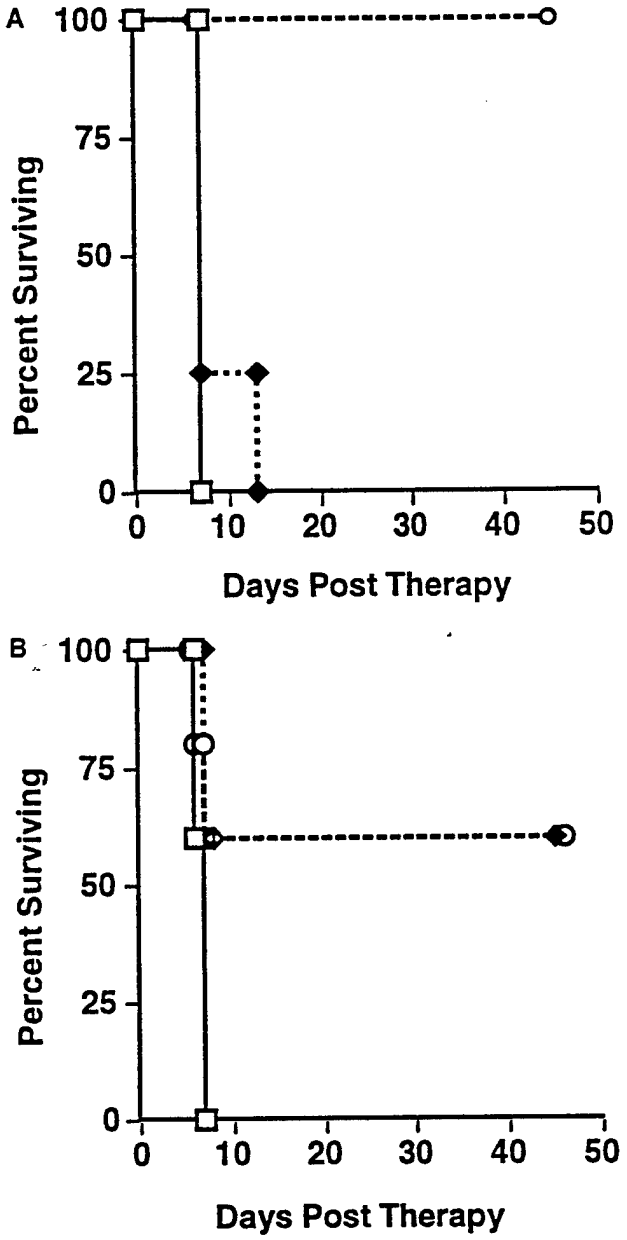

FIG. 1. Survival of SK-OV-3 tumor-bearing nude mice following therapy with ^{213}Bi-labeled CHX-A″-C6.5K-A single-chain Fv (scFv) or diabody. (A) Mice receiving 1.1 μCi (squares), 0.6 μCi (diamonds), or 0.3 μCi (circles) of ^{213}Bi-labeled CHX-A″-C6.5K-A scFv. (B) Mice receiving 0.64 μCi (squares), 0.4 μCi (diamonds), or 0.15 (circles) μCi of ^{213}Bi-labeled CHX-A″-C6.5K-A diabody. N = 5 mice per group.

Based on the above results, a second therapy study focused exclusively on ^{213}Bi-labeled scFv constructs. In this trial mice bearing established SK-OV-3 tumors (mean tumor size = 16.6 ± 8.1 mm^3) were treated with a single intravenous injection of ^{213}Bi-labeled CHX-A″ conjugated to either the anti-HER2/*neu* C6.5K-A scFv (10 mice per treatment group) or the irrelevant control NM3E2 scFv (5–6 mice per treatment group). Separate groups were treated with either 300 μCi (166–340 μg) or 150 μCi (83–110 μg) of ^{213}Bi-labeled CHX-A″ conjugated to each scFv.

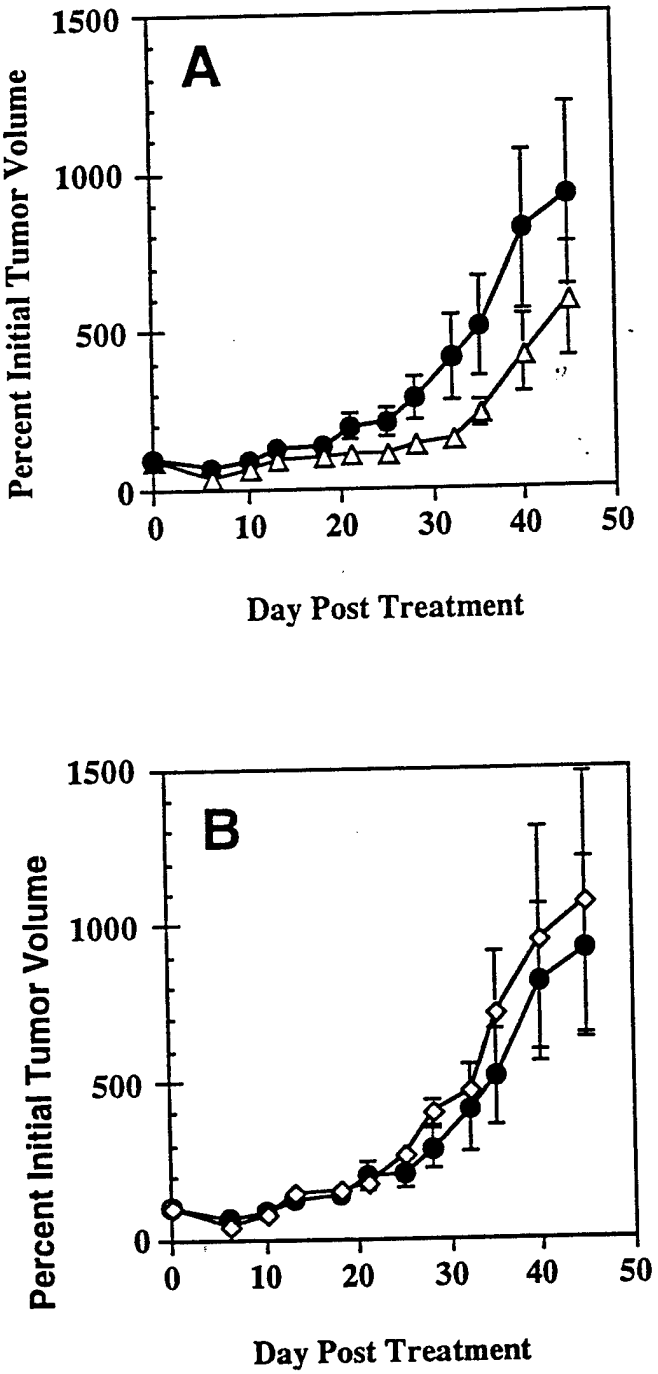

FIG. 2. ^{213}Bi-labeled CHX-A″-C6.5K-A diabody and single-chain Fv (scFv) therapy of early tumors. Nude mice with small palpable (10 days postimplantation) SK-OV-3 ovarian carcinoma tumors were treated with a single intravenous dose of (A) 0.15 μCi ^{213}Bi-labeled CHX-A″-C6.5K-A scFv (triangles) or (B) 0.30 μCi ^{213}Bi-labeled CHX-A″-C6.5K-A diabody (diamonds). Untreated control mice (circles) are included in each graph. Results are presented as the percent of initial tumor volume (mm^3). N = 5 mice per group. Two mice in the diabody treatment group died from treatment-related toxicity prior to day 7 following therapy. SEMs are indicated.

Control mice were treated with 80 μg of unconjugated (cold) C6.5K-A scFv. As evidenced by weight loss, only minimal treatment-associated toxicity was observed in this study (−3.4% and −9.9% for the 150 μCi and 300 μCi groups, respectively). A single 150 μCi dose of ^{213}Bi conjugated to either the C6.5K-A or NM3E2 scFvs did not significantly impact the rate of tumor growth compared with control mice treated with unlabeled C.5 scFv (p = 0.1124 and 0.5152; Fig. 3). Increasing the dose to 300 μCi of ^{213}Bi-labeled CHX-A″-C6.5K-A scFv resulted in a significantly decreased tumor growth rate compared with the controls treated with unlabeled C6.5K-A scFv (p = 0.0032; Fig. 3). However, because similar growth delays resulted from treatment with 300 μCi of ^{213}Bi using both the anti-Her2/*neu* and irrelevant scFv vehicles (p = 0.4624), the observed effects were not tumor-specific. The growth plots corresponding to individual tumors are provided in Figure 4.

DISCUSSION

Many major obstacles to the success of RAIT have been overcome. In particular, the field of chelation chemistry has provided new agents that have very high affinities for a variety of radiometals. One such molecule, CHX-A″ DTPA, was employed in this study. The CHX-A″ DTPA is a versatile chelator that has been shown to bind radiometals such as ^{111}In, ^{90}Y, and ^{212}Bi or ^{213}Bi with excellent stability and suitable formation kinetics to obviate radiolysis effects (20). This has allowed us to perform biodistribution studies with ^{111}In-CHX-A″-labeled scFv and diabody to predict tumor-specific distributions that would be achieved with the shorter-lived, and more difficult to track, α-emitter ^{213}Bi (data not shown).

The small size of scFv molecules leads to their rapid renal elimination. When these molecules are labeled with radioiodine, dehalogenation occurs and the iodine is excreted in the urine. However, a very different pattern of renal retention occurs when a radiometal is employed as a trace or therapeutic label on an scFv molecule. In a study comparing the metabolic patterns of ^{125}I and ^{177}Lu labeled scFv, Schott *et al.* (32) observed that significantly greater renal and reticuloendothelial retention was associated with the use of radiometals. Similar observations have been made by a number of groups when larger Fab fragments are employed in place of scFv molecules (9, 27).

Recently a number of groups have described the utility of employing doses of cationic amino acids to decrease the renal retention of radiolabeled antibody fragments (6, 7, 9, 27). Prior to initiating the current study, we evaluated the utility of using intraperitoneal injections of L-lysine to achieve similar results with ^{111}In-labeled CHX-A″-C6.5K-A diabody (data not shown). We did not achieve the five- to sixfold reduction in renal uptake that was observed by Behr *et al.* (6) when L-lysine was administered prior to ^{125}I-Fab′. However, we did observe significant decreases in renal retention in the presence of L-lysine without altering the tumor-targeting properties of the radiolabeled diabody. Accordingly, we decided to preadminister L-lysine in the therapy/MTD studies to reduce the potential for renal toxicity.

This is the first report of the use of α-emitting radioisotopes with engineered antibody fragments. α-Emitting radioisotopes have a number of properties that make them highly attractive for RAIT applications. These include a high linear energy transfer (LET) and a high relative biological effectiveness for cell kill stemming from the inability of cells to repair damage resulting from α-particle transversal (34). The therapeutic potential of α emitters is apparent when they are compared with commonly employed β emitters. One

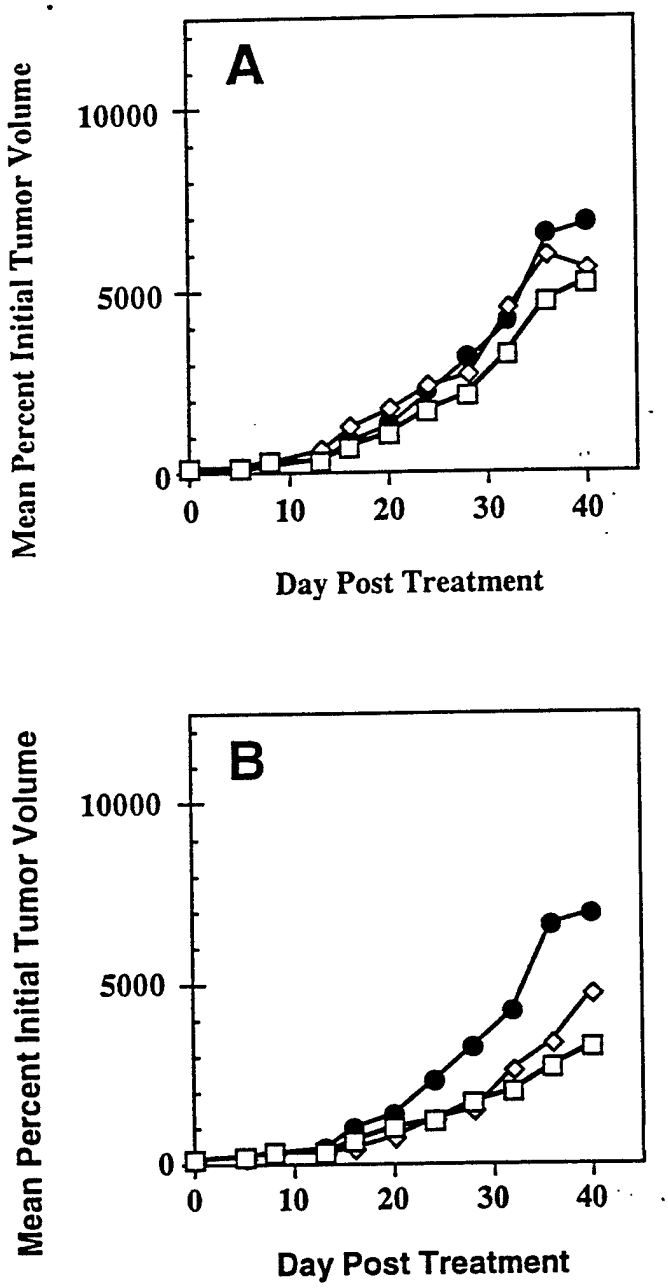

FIG. 3. ^{213}Bi-labeled CHX-A″-C6.5K-A single-chain Fv (scFv) therapy of established tumors. Nude mice bearing large (mean = 16.6 ± 18.1 mm^3) SK-OV-3 tumors were treated with (A) 0.15 μCi or (B) 0.3 μCi of ^{213}Bi conjugated to C6.5K-A scFv (squares) or to NM3E2 scFv (diamonds), an irrelevant control specific for CD16. Control mice treated with unlabeled C6.5K-A scFv (circles) are included in each graph. Results are presented as the mean percent of initial tumor volume (mm^3) for each group. N = 10 mice for all C6.5K-A groups and 6 and 5 mice, respectively, for the low- and high-dose NM3E2 groups. Graphs detailing individual mice are presented in Figure 4.

of the most promising β emitters employed in RAIT is ^{90}Y, which has a LET of 0.2 keV/μm and a mean range in tissue of approximately 4 mm. In contrast, the most attractive α emitters (^{211}At and ^{213}Bi) have an approximately 500-fold greater LET (approximately 100 keV/μm) and a 55-fold shorter mean range in tissue (70 μm) (22). When employed in targeted therapy, this translates into significantly greater specificity and efficiency of effect. Furthermore, unlike the situation with β particles, the presence of oxygen is not required for α-particle–based cell killing. Hence, they can be effective even in hypoxic regions of tumors. However, whereas β-emitting isotopes have been extensively employed in RAIT, α-emitting isotopes have largely been bypassed, primarily due to half-life imposed difficulties inherent in their production and shipping. The recent development of generators for the production of α emitters, such as the ^{225}Ac/^{213}Bi generator we employed here (37), has overcome the major hurdle to their use.

To date, short-lived α-emitter (e.g., ^{213}Bi, ^{212}Bi, or ^{211}At)-based RAIT has been most effective when employed in preclinical trials to treat tumors that are in a defined compartment, accessible through regional delivery of the radiopharmaceutical, or readily accessible from the circulation. Examples of regional approaches include the successful treatment of intraperitoneal EL-4 ascites tumors with ^{212}Bi-labeled IgM specific for Thy 1.2 by Macklis *et al.* (21) and the prolonged survival of mice bearing intraperitoneal LS174T colon carcinoma following treatment with ^{212}Bi-labeled B72.3 MAb (33). The potential of α-emitter–based RAIT of targets that are readily accessible to the circulation has been demonstrated in leukemia models in mice (22, 26) and in studies by Kennel and Mirzadeh (18) that targeted vascular cells to treat adjacent lung tumors. In the latter model, treatment of mice with ^{213}Bi-labeled MAb 201B, specific for murine thrombomodulin, extended the life span of mice bearing multiple small (50–400 cell) EMT-6 lung tumors. Accordingly, a major goal of the present study was to determine if the pairing of a short-lived α emitter with a rapidly localized (and cleared) targeting agent could extend the utility of this class of isotopes to the treatment of solid subcutaneous tumors.

The studies presented here indicate that ^{213}Bi can be conjugated successfully to the scFv and diabody molecules via the CHX-A″ chelate. Our preliminary preclinical therapy trials demonstrated that significant reductions in the growth rates of early and established human tumor xenografts could be achieved by treating the mice with 0.3 μCi of ^{213}Bi chelated to the anti-HER2/*neu* scFv C6.5K-A. However, we observed similar results when the ^{213}Bi was conjugated to an irrelevant control scFv, suggesting that the anti-tumor effects were nonspecific in nature. This is consistent with the observation that both scFv molecules display similar pharmacokinetics (data not shown) and with our previously published results that reported significant tumor localization of both anti-tumor and irrelevant scFv 1 h postinjection (2). Because both molecules had potentially similar early (nonspecific) tumor and vascular levels, it is not surprising that they displayed equal anti-tumor effects when combined with short-lived, short track-length isotopes. Alternatively, the lack of a tumor-specific therapeutic effect could result from instability of the scFv and diabody molecules *in vivo*. However, we believe this to be extremely unlikely because the *in vivo* tumor targeting properties of both molecules have been fully characterized in a similar model system using ^{125}I- (3, 4, 30) and ^{111}In-labeled CHX-A″ chelate-conjugation (unpublished data) strategies.

The ability of the α particles to penetrate tissues (70 μm average track length) is very short compared with the tumor radii (ranging from 5–8 mm and 2–3 mm in the first and second studies, respectively). Thus, it is likely that the observed decrease in tumor growth rate resulted from exposures received by tumor vasculature, neovasculature, and tumor cells in the immediate vicinity of the blood vessels. However, in light of the nonspecific nature of current chemotherapeutic drugs, an effective radiopharmaceutical with a

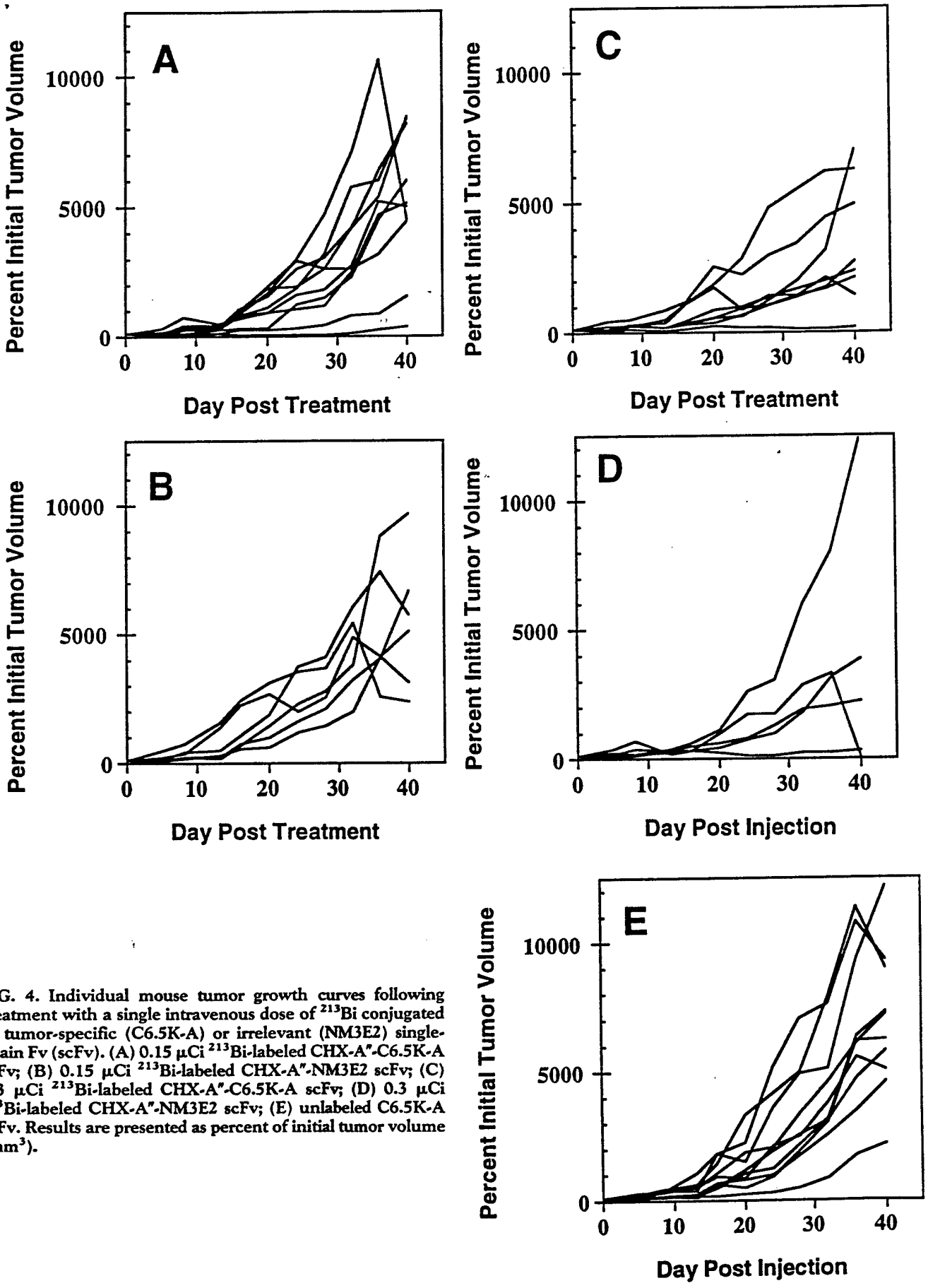

FIG. 4. Individual mouse tumor growth curves following treatment with a single intravenous dose of ^{213}Bi conjugated to tumor-specific (C6.5K-A) or irrelevant (NM3E2) single-chain Fv (scFv). (A) 0.15 μCi ^{213}Bi-labeled CHX-A″-C6.5K-A scFv; (B) 0.15 μCi ^{213}Bi-labeled CHX-A″-NM3E2 scFv; (C) 0.3 μCi ^{213}Bi-labeled CHX-A″-C6.5K-A scFv; (D) 0.3 μCi ^{213}Bi-labeled CHX-A″-NM3E2 scFv; (E) unlabeled C6.5K-A scFv. Results are presented as percent of initial tumor volume (mm^3).

combination of specific and nonspecific targeting components has advantages over the status quo.

In light of the results presented here, it is clear that more effort must be expended to match the physical half-lives of therapeutic isotopes with the biological properties of their delivery vehicles. For example, with a β half-life (elimination rate from circulation) of 5.7 h and a tumor retention half-life of nearly 24 h, the C6.5 diabody could be effectively paired with either ^{90}Y or ^{211}At, which have half-lives of 64 and 7.2 h, respectively. Furthermore, the best use of the short-lived ^{213}Bi may be in antibody pretargeting applications where the isotope-chelate complexes have elimination half-lives on the order of 30 min.

In conclusion, although scFv-targeted short-lived α emitters can mediated tumor growth delays, the majority of their effects are likely not dependent on the specificity of the targeting vehicle. Utilization of isotopes with half-lives that more closely match the pharmacokinetic and tumor retention profiles of the delivery vehicle should significantly improve the specificity of therapeutic effects.

References

1. Adams G. P., DeNardo S. J., Deshpande S. V., DeNardo G. L., Meares C. F., McCall M. J. and Epstein A. L. (1989) Effect of mass of ^{111}In-benzyl-EDTA monoclonal antibody on hepatic uptake and processing in mice. *Cancer Res.* **49**, 1707–1711.
2. Adams G. P., McCartney J. E., Tai M.-S., Oppermann H., Huston J. S., Stafford W. F., Bookman M. A., Fand I., Houston L. L. and Weiner L. M. (1993) Highly specific *in vivo* tumor targeting by monovalent and divalent forms of 741F8 anti-c-erbB-2 single-chain Fv. *Cancer Res.* **53**, 4026–4034.
3. Adams G. P., Schier R., Marshall K., Wolf E. J., McCall A. M., Marks J. D. and Weiner L. M. (1998) Increased affinity leads to improved selective tumor delivery of single chain Fv antibodies. *Cancer Res.* **58**, 485–490.
4. Adams G. P., Schier R., McCall A. M., Crawford R. S., Wolf E. J., Weiner L. M. and Marks J. D. (1998) Prolonged *in vivo* tumor retention of a human diabody targeting the extracellular domain of human HER2/neu. *Brit. J. Cancer* **77**, 1405–1412.
5. Alpaugh K. and von Mehren M. (1999) Monoclonal antibodies in cancer treatment. *BioDrugs* **3**, 209–236.
6. Behr T. M., Goldenberg D. M. and Becker W. (1998) Reducing renal accretion of radiolabelled antibody fragments and peptides: Improvement of therapeutic efficacy by overcoming nephrotoxic potential? A review. *Tumor Targeting* **3**, 2–12.
7. Behr T. M., Sharkey R. M., Malik J. E., Blumenthal R. D., Dunn R. M., Griffiths G. L., Bair H.-J., Wolf F. G., Becker W. S. and Goldenberg D. M. (1995) Reduction of the renal uptake of radiolabeled monoclonal antibody fragments by cationic amino acids and their derivatives. *Cancer Res.* **55**, 3825–3834.
8. Colcher D. R., Bird R., Roselli M., Hardman K. D., Johnson S., Pope S., Dodd S. W., Pantoliáno M. W., Milenic D. E. and Schlom, J. (1990) In vivo tumor targeting of a recombinant single-chain antigen-binding protein. *J. Natl. Cancer Inst.* **82**, 1191–1197.
9. DePalatis L. R., Frazier K. A., Cheng R. C. and Kotite N. J. (1995) Lysine reduces renal accumulation of radioactivity associated with injection of the [^{177}Lu]α-[2-(4-aminophenyl) ethyl]-1,4,7,10-tetraazacyclodecane-1,4,7,10-tetraacetic acid-CC49 immunoconjugate. *Cancer Res.* **55**, 5288–5295.
10. Feinendegen L. E. and McClure J. J. (1997) Alpha-emitters for medical therapy—Workshop of the United States Department of Energy (meeting report) *Radiat. Res.* **148**, 195–201.
11. Feinendegen L. E. and McClure J. J. (1999) Alpha emitters for medical therapy: Second Bi-annual Workshop. Toronto, Canada. June 4–5, 1998. USA Dept. of Energy Publication DOE/NE-0116.
12. Hann H.-W. L., Stahlhut M. W., Rubin R. and Maddrey W. C. (1992) Antitumor effect of deferoxamine on human hepatocellular carcinoma growing in athymic nude mice. *Cancer* **70**, 2025–2056.
13. Hollinger P., Prospero T. and Winter G. (1993) "Diabodies": Small bivalent and bispecific antibody fragments. *Proc. Natl. Acad. Sci. USA* **90**, 6444–6448.
14. Huston J. S., Levinson D., Mudgett-Hunter M., Tai M.-S. and Novotny J. (1988) Protein engineering of antibody binding sites: Recovery of specific activity in an anti-digoxin single-chain Fv analogue produced in *E coli*. *Proc. Natl. Acad. Sci. USA* **85**, 5879–5883.
15. Jain R. K. (1993) Physiological resistance to the treatment of solid tumors. Fourth Annual IBC International Conference on Antibody Engineering. **4**, 87–105.
16. Jain R. K. (1987) Transport of molecules in the tumor interstitum: A review. *Cancer Res.* **47**, 3039–3051.
17. Kaminski M. S., Zasady K. R., Francis I. R., Milik A. W., Ross C. W., Moon S. D., Crawford S. M., Burgess J. M., Petry N. A., Butchko G. M., Glenn S. D. and Wahl R. L. (1993) Radioimmunotherapy of B-cell lymphoma with ^{131}I-anti-B1 (anti-CD20) antibody. *New Engl. J. Med.* **329**, 459–465.
18. Kennel S. J. and Mirzadeh S. (1998) Vascular targeted radioimmunotherapy with ^{213}Bi—an α-particle emitter. *Nucl. Med. Biol.* **25**, 241–246.
19. Knox S. J., Goris M. L., Trisler K., Negrin R., Davis T., Liles T. M., Grillo-Lopez A., Chinn P., Varns C., Ning S. C., Fowler S., Deb N., Becker M., Marquez C. and Levy R. (1996) Yttrium-90-labeled anti-CD20 monoclonal antibody therapy of recurrent B-cell lymphoma. *Clin. Cancer Res.* **2**, 457–470.
20. Kobayashi H., Wu C., Yoo T. M., Sun B. F., Drumm D., Pastan I., Paik C. H., Gansow O. A., Carrasquillo J. A. and Brechbiel M. W. (1998) Evaluation of the *in vivo* biodistribution of yttrium-labeled isomers of CHX-DTPA-conjugated monoclonal antibodies. *J. Nucl. Med.* **39**, 829–836.
21. Macklis R. M., Kinsey B. M., Kassis A. L., Ferrara J. L. M., Atcher R. W., Hines J. J., Coleman C. N., Adelstein S. J. and Burackoff S. J. (1988) Radioimmunotherapy with alpha-emitting immunoconjugates. *Science* **240**, 1024–1026.
22. McDevitt M. R., Sgouros G., Finn R. D., Humm J. L., Jurcic J. G., Larson S. M. and Scheinberg D. A. (1998) Radioimmunotherapy with alpha-emitting nuclides. *Eur. J. Nucl. Med.* **25**, 1341–1351.
23. Meares C. F., McCall M. J., Reardan D. T., Goodwin D. A., Diamanti C. I. and McTigue M. (1984) Conjugation of antibodies with bifunctional chelating agents: Isothiocyanate and bromoacetamide reagents, methods of analysis, and subsequent addition of metal ions. *Anal. Biochem.* **142**, 68–78.
24. Milenic D. E., Yokota T., Filpula D. R., Finkelman M. A. J., Dodd S. W., Wood J. F., Whitlow M., Snoy P. and Schlom J. (1991) Construction, binding properties, metabolism, and targeting of a single-chain Fv derived from the pancarcinoma monoclonal antibody CC49. *Cancer Res.* **51**, 6363–6371.
25. Mirzadah S., Brechbiel M. W., Atcher R. W. and Gansow O. A. (1990) Radiometal labeling of immunoproteins: Covalent linkage of 2-(4-isothiocyanatobenzyl) diethylenetriaminepentaacetic acid ligands to immunoglobulin. *Bioconjug. Chem.* **1**, 59–65.
26. Nikula T. K., McDevitt M. R., Finn R. D., Wu C., Kozak R. W., Garmestani K., Brechbiel M. W., Curcio M. J., Pippin C. G., Tiffany-Jones L., Geerlings M. W. Sr., Apostolidis C., Molinet R., Geerlings M. W. Jr., Gansow O. A. and Scheinberg, D. A. (1999) Alpha-emitting bismuth cyclohexylbenzyl DTPA constructs of recombinant humanized anti-CD33 antibodies: Pharmacokinetics, bioactivity, toxicity and chemistry. *J. Nucl. Med.* **40**, 166–176.
27. Pimm M. V. and Gribben S. J. (1994) Prevention of renal tubule re-absorption of radiometal (indium-111) labelled Fab fragment of a monoclonal antibody in mice by systemic administration of lysine. *Eur. J. Nucl. Med.* **21**, 663–665.
28. Pippin C. G., Parker T. A., McMurry T. J. and Brechbiel M. W. (1992) Spectrophotometric method for the determination of a bifunctional DTPA ligand in DTPA-monoclonal antibody conjugates. *Bioconjug. Chem.* **3**, 342–345.
29. Press O. W., Eary J. F., Appelbaum F. R., Martin P. J., Badger C. C., Nelp W. B., Glenn S., Butchko G., Fisher D., Porter B., Matthews D. C., Fischer L. D. and Bernstein I. D. (1993) Radiolabeled-antibody therapy of B-cell lymphoma with autologous bone marrow support. *New Engl. J. Med.* **329**, 1219–1224.
30. Schier R., Marks J. D., Wolf E. J., Apell G., Wong C., McCartney J. E., Bookman M. A., Huston J. S., Houston L. L., Weiner L. M. and Adams G. P. (1995) *In vitro* and *in vivo* characterization of a human anti-c-erbB-2 single-chain Fv isolated from a filamentous phage antibody library. *Immunotechnology* **1**, 73–81.
31. Schier R., McCall A., Adams G. P., Marshall K. W., Merritt H., Yim M., Crawford R. S., Weiner L. M. and Marks J. D. (1996) Isolation of picomolar affinity anti-c-erbB-2 single-chain Fv by molecular evolution

of the complementarity determining regions in the center of the antibody binding site. *J. Mol. Biol.* **263**, 551–567.
32. Schott M. E., Milenic D. E., Yokota T., Whitlow M., Wood J. F., Fordyce W. A., Cheng R. C. and Schlom J. (1992) Differential metabolic patterns of iodinated versus radiometal chelated anti-carcinoma single-chain Fv molecules. *Cancer Res.* **52**, 6413–6417.
33. Simonson R. B., Ultee M. E., Hauler J. A. and Alvarez V. L. (1990) Radioimmunotherapy of peritoneal human colon cancer xenografts with site-specifically modified Bi-212-labeled antibody. *Cancer Res.* **50**, 985s–988s.
34. Wilbur D. S. (1991) Potential use of alpha emitting radionuclides in the treatment of cancer. *Antibody, Immunoconj. Radiopharm.* **4**, 85–97.
35. Wu A. M., Chen W., Raubitschek A. A., Willams L. E., Fischer R., Hu S.-Z., Odom-Maryon T., Wong J. Y. C. and Shively J. E. (1996) Tumor localization of anti-CEA single chain Fvs: Improved targeting by non-covalent dimers. *Immunotechnology* **2**, 21–36.
36. Wu A. M., Wiliams L. E., Zieran L., Padma A., Sherman M., Bebb G. G., Odom-Maryon T., Wong J. Y. C., Shively J. E. and Raubitschek A. A. (1999) Anti-carcinoembryonic antigen (CEA) diabody for rapid tumor targeting and imaging. *Tumor Targeting* **4**, 47–58.
37. Wu C., Brechbiel M. W. and Gansow O. A. (1997) An improved generator for the production of ^{213}Bi from ^{225}Ac. *Radiochim. Acta* **79**, 141–144.
38. Wu C., Kobayashi H., Sun B., Yoo T. M., Paik C. H., Gansow O. A., Carrasquillo J. A., Pastan I. and Brechbiel M. W. (1997) Stereochemical influence on the stability of radio-metal complexes *in vivo*. Synthesis and evaluation of the four stereoisomers of 2-(*p*-nitrobenzyl)-trans-CyDTPA. *Bioorg. Med. Chem.* **5**, 1925–1934.

ELSEVIER

Journal of Immunological Methods 251 (2001) 123–135

JIM
Journal of Immunological Methods

www.elsevier.nl/locate/jim

Recombinant Technology

Expression of single-chain Fv-Fc fusions in *Pichia pastoris*

David B. Powers[a], Peter Amersdorfer[a,b], Marie-Alix Poul[a,c], Ulrik B. Nielsen[a], M. Refaat Shalaby[d], Gregory P. Adams[e], Louis M. Weiner[e], James D. Marks[a,*]

[a]*Departments of Anesthesia and Pharmaceutical Chemistry, University of California San Francisco, San Francisco, CA 94110, USA*
[b]*Phylos Inc., 128 Spring Street, Lexington, MA 02421, USA*
[c]*UMR CNRS 8532, Laboratoire de Biotechnologies et de Pharmacogénétique Appliquée, Ecole Normale Superieure de Cachan, 61 avenue du President Wilson, 94235 Cachan Cedex, France*
[d]*California Pacific Medical Center, San Francisco, CA 94115, USA*
[e]*Department of Medical Oncology, Fox Chase Cancer Center, Philadelphia, PA 19111, USA*

Received 22 September 1999; received in revised form 23 August 2000; accepted 23 August 2000

Abstract

Phage display technology makes possible the direct isolation of monovalent single-chain Fv antibody fragments. For many applications, however, it is useful to restore Fc mediated antibody functions such as avidity, effector functions and a prolonged serum half-life. We have constructed vectors for the convenient, rapid expression of a single-chain antibody Fv domain (scFv) fused to the Fc portion of human IgG1 in the methylotrophic yeast *Pichia pastoris*. The scFv-Fc fusion protein is secreted and recovered from the culture medium as a disulfide-linked, glycosylated homodimer. The increased size of the dimer (~106 kDa vs. ~25 kDa for a scFv) results in a prolonged serum half-life in vivo, with $t_{1/2}$ of the beta phase of clearance increasing from 3.5 h for a typical scFv to 93 h for a scFv-Fc fusion in mice. The scFv-Fc fusion is capable of mediating antibody-dependent cellular cytotoxicity against tumor target cells using human peripheral blood mononuclear cells as effectors. Finally, the Fc domain is a convenient, robust affinity handle for purification and immunochemical applications, eliminating the need for proteolytically sensitive epitope and/or affinity tags on the scFv.

Keywords: Pichia pastoris; scFv; Antibody engineering; Phage display; HER2/neu; Botulism

Abbreviations: Fv, antibody variable fragment; scFv, single chain Fv fragment; kDa, kilodaltons; V_H, immunoglobulin heavy chain variable region; V_L, immunoglobulin light chain variable region; C_H2 and C_H3, immunoglobulin heavy chain constant regions 2 and 3; ADCC, antibody-dependent cellular cytotoxicity; PCR, polymerase chain reaction; BoNT, botulinum neurotoxin; BoNT/A, BoNT type A; H_c, BoNT binding domain; ELISA, enzyme linked immunosorbent assay; SDS–PAGE, sodium dodecyl sulfate–polyacrylamide gel electrophoresis; HRP, horse radish peroxidase; AMP, ampicillin; KAN, kanamycin; ZEO, Zeocin; PBS, phosphate buffered saline (25 mM NaH_2PO_4, 125 mM NaCl, pH 7.4); MPBS, 2% milk powder in PBS; FACS, fluorescence activated cell sorting; FITC, fluorescein isothiocyanate; PE, phycoerythrin; PBMC, peripheral blood mononuclear cells; RU, resonance units; ECD, extracellular domain; HBS, hepes buffered saline (10 mM Hepes, 150 mM NaCl, pH 7.4); k_{off}, dissociation rate constant; k_{on}, association rate constant; M_r, molecular weight; RT, room temperature; YNB, yeast nitrogen base (with ammonium sulfate without amino acids); i.v., intravenous; i.p., intraperitoneal.

*Corresponding author. San Francisco General Hospital, Room 3C-38, 1001 Potrero Avenue, San Francisco CA, 94110 USA. Tel.: +1-415-206-3256; fax: +1-415-206-3253.
E-mail address: marksj@anesthesia.ucsf.edu (J.D. Marks).

0022-1759/01/$ – see front matter
PII: S0022-1759(00)00290-8

1. Introduction

The modular nature of antibody molecules allows for an almost unlimited number of domain rearrangements and fusions. Antibody engineering allows the researcher to design and use a variety of binding domains, effector domains, as well as non-antibody fusion partners (Chamow and Ashkenazi, 1999; Hoogenboom, 1997). One of the most useful antibody fragments is the single-chain Fv (scFv) in which the isolated antibody V_H and V_L domains are joined by a short peptide linker (Bird et al., 1988; Huston et al., 1988). This monovalent, minimal binding fragment is favored for antibody phage display techniques and phage antibody library construction (Marks et al., 1991; McCafferty et al., 1990).

Once a scFv has been isolated from a phage display library, the binding domain can be characterized with respect to affinity, epitope, and biological activity, as well as subjected to further affinity maturation. The scFv can be used as is, or engineered into other formats (Fv, Fab, $(Fab')_2$, IgG, or fused to other proteins).

For some applications the scFv itself is the desired format. The small size of the scFv, its rapid clearance from the blood, and tumor penetration properties make it the format of choice for tumor targeting and radioimmunoimaging applications (Adams et al., 1995; Adams et al., 1998; Yokata et al., 1992). The single-chain nature of the scFv is also best-suited for intracellular immunization (intrabody) applications (Marasco, 1997). However for other uses, it would be desirable to transfer the antigen-binding properties of the scFv into a full length IgG, to take advantage of avidity effects, effector functions, and the prolonged serum half-life of an immunoglobulin. Increasing the serum half-life of scFv is particularly important for efficient in vivo antigen neutralization since the $t_{1/2}\beta$ of a typical scFv is only 3.5 h in mice (Huston et al., 1996).

One approach is to directly engineer a phage displayed scFv into a full length IgG and express it in mammalian cells (Persic et al., 1997). However this approach requires separate cloning steps for the V_H and V_L domains, and establishing a stable antibody secreting cell line can be time consuming. An alternate approach would be to engineer the scFv into a more 'IgG-like' structure that can be accomplished in a single cloning step, and that can be expressed at high levels in a eucaryotic microorganism such as yeast. We have constructed a vector to rapidly express an scFv-Fc fusion (wherein the scFv is fused to the hinge, C_H2, and C_H3 domains of human IgG1) in the methylotrophic yeast *Pichia pastoris*. The scFv-Fc fusion can easily be constructed in a single cloning step from a scFv and is secreted at high levels as a glycosylated dimer from *Pichia* cultures. The scFv-Fc fusion retains the affinity and specificity of the parent scFv, combined with the bivalency, prolonged serum half-life, and the Fc-mediated ADCC (antibody-dependent cellular cytotoxicity) of an IgG. These yeast-produced scFv-Fc fusions will be useful to rapidly characterize candidate scFv isolated from phage antibody libraries before converting to a full-length IgG, or as an alternative format in its own right.

2. Materials and methods

2.1. Cells and media

Pichia pastoris strain GS115 was obtained from Invitrogen, San Diego, CA. SKBR-3 and SK-OV-3 cells were obtained from the ATCC (American Type Culture Collection, Rockville, MD). Media used: YPD, yeast extract peptone dextrose medium (1% yeast extract, 2% peptone, 2% dextrose); YPDS, YPD medium plus 1 M sorbitol; BMGY, buffered glycerol complex medium (1% yeast extract, 2% peptone, 100 mM phosphate buffer pH 6.0, 1.34% YNB, 4×10^{-5}% biotin, 1% glycerol); BMMY, buffered methanol complex medium (1% yeast extract, 2% peptone, 100 mM phosphate buffer pH 6.0, 1.34% YNB, 4×10^{-5}% biotin, 0.5% methanol).

2.2. pPIgG1, pPIgG1-C25, and pPIgG1-C6.5 plasmid construction

The Fc fragment (hinge, C_H2 and C_H3) of human IgG1 was amplified from the baculovirus expression plasmid pBHuCγ1 (Poul et al., 1995) using primers 'HulgG*Not*Iback' (5′-AAGGAAAAA*GCGGCC-GC*AGAGCCCAAATCTTGTGACAAA-3′) and 'HuIgG*Xba*Ifor' (5′-ACGC*TCTAGA*TCATTTACC-

CGGAGACAGGGAC-3′), which append *Not*I and *Xba*I sites (underlined) onto the 5′ and 3′ ends of the PCR fragment, respectively. The PCR fragment was digested with *Not*I and *Xba*I and subcloned into *Not*I-*Xba*I digested pPICZαA (Invitrogen) to generate plasmid pPIgG1 (for 'Pichia IgG plasmid 1').

C25, a scFv which binds the botulinum neurotoxin type A binding domain (BoNT/A Hc) (Amersdorfer et al., 1997) was PCR amplified from vector pUC119MycHis-C25 using primers 'C25PichiaBack' (5′-CGGCAG*CTCGAG*AAAAGAGAGGCTGAAG-CTCAGGTCCAGCTGCAGGAGTCTGGG-3′) and 'LMB2' (5′-GTAAAACGACGGCCAGT-3′). The 5′ PCR primer C25PichiaBack appends a *Xho*I site (underlined) onto the 5′ end of the scFv for cloning into the *Xho*I site in the leader sequence of plasmid pPIgG1, and also recreates the last few amino acids of the leader sequence fused with the first codon of the C25 scFv. The 3′ PCR primer LMB2 anneals outside of a unique *Not*I site at the end of the C25 scFv, derived from plasmid pHEN1 (Hoogenboom et al., 1991). The PCR fragment was then digested with *Xho*I and *Not*I and subcloned into *Xho*I and *Not*I digested plasmid pPIgG1 generating plasmid pPIgG1-C25. Similarly, C6.5, a scFv which binds the extracellular domain of the HER2/*neu* oncoprotein (Schier et al., 1995) was subcloned into pPIgG1 using primers 'C6.5PichiaBack' (5′-CGGCAG*CKC-GAG*AAAAGAGAGGCTGAAGCTGGCCAGGTG-CAGCTGGTGCAG-3′) and 'LMB2' to create plasmid pPIgG1-C6.5. Following construction, the coding sequences for the Fc region and both the scFvs were sequenced to exclude any PCR-induced errors.

2.3. Electroporation

Pichia pastoris strain GS115 was transformed by electroporation. 10 μg of plasmid was linearized with *Pme*I, phenol-chloroform extracted, ethanol precipitated, and dissolved in 10 μl of dH_2O. Preparation of electrocompetent *Pichia* strain GS115 was done as per supplier's instructions (Invitrogen). 80 μl of electrocompetent cells were mixed with 5-10 μg of linearized plasmid in a 0.2 cm electroporation cuvette, incubated on ice 5 min, and electroporated in a Biorad GenePulser with settings of 1500 V, 25 uF capacitance, and 400 ohms resistance. After pulsing, 1.0 ml of ice cold 1 M sorbitol was added immediately to the cuvette, and the cells transferred to a sterile 15 ml culture tube. The tube was incubated at 30°C without shaking for 1 h, then 1.0 ml YPD medium was added to the tube, and the cells were allowed to recover for 2 h at 30°C at 250 RPM. Transformants were plated (200 μl) on YPDS plates containing 100 μg/ml Zeocin and grown at 30°C to isolate Zeocin-resistant transformants.

2.4. Small scale expression and screening of Pichia transformants

Zeocin-resistant transformants of pPIgG1-C25, pPIgG1-C6.5 and pPICZαA (control) plasmids were grown overnight in BMGY medium at 30°C and 250 rpm shaking in 100 ml glass culture tubes. The next day, the cells were recovered by centrifugation and resuspended to an OD_{600} of 1.0 in BMMY media to induce, and grown again at 30°C and 250 rpm. Fresh methanol was added to a total of 0.5% to maintain induction at 24, 48 and 72 h post induction. After 72 h, samples of the media were analyzed by SDS–PAGE followed by silver stain (Biorad Silver Stain Plus, Biorad, Hercules, CA) and Western blot with polyclonal goat anti-human IgG (Fc-specific) conjugated to horse radish peroxidase (A-0170, Sigma, St. Louis, MO). Detection was with the chemiluminescent substrate ECL (Amersham Pharmacia Biotech, Piscataway, New Jersey).

2.5. Large scale expression and purification of scFv-Fc fusions

250 ml cultures of GS115/pPIgG1-C25 and GS115/pPIgG1-C6.5 were grown overnight in BMGY plus Zeocin (50 μg/ml) and kanamycin (50 μg/ml) until the OD_{600} was 4–6. The cells were recovered by centrifugation, then diluted to an OD_{600} of 1.0 in 1000 ml of fresh BMMY media containing 50 μg/ml kanamycin to induce. The 1000 ml of resuspended cells were divided equally between 4×2 l baffle-bottom flasks to ensure adequate aeration, and grown at 30°C and 250 rpm. Fresh methanol was added to 0.5% to maintain induction at 24, 48, and 72 h. After 72 h, the cells were removed by centrifugation and the scFv-Fc fusion protein purified from the supernatant. Twenty five milliliters of a protease inhibitor cocktail (P2714, Sigma) was added

to reduce proteolysis, and the pH of the supernatant was adjusted to 8.0 by the addition of 1/10 volume of 1.0 M Tris pH 8.0. Proteins were precipitated by the addition of 400 g ammonium sulfate in the cold with constant stirring over a period of 2 h. The precipitate was recovered by centrifugation, dissolved in 40 ml of 25 mM Tris pH 8.0, and dialyzed overnight against two changes of 4 l apiece of 25 mM Tris pH 8.0 at 4°C. After dialysis, the sample was applied to a 1.5 ml Protein G column (Sigma) that had been previously equilibrated with 25 mM Tris pH 8.0. The column was washed once with 10 ml of 100 mM Tris pH 8.0, once with 10 ml of 10 mM Tris pH 8.0, and eluted with 20 ml of 100 mM glycine pH 3.0. 1.0 ml fractions were collected in Eppendorf tubes containing 100 μl of 1.0 M Tris pH 8.0 to neutralize. Peak fractions were determined by absorbance at 280 nm, pooled, concentrated to 0.5 ml on a Centricon 10 concentrator (Amicon, Beverley, MA) and finally gel filtered on a Superdex S-200 column (Amersham Pharmacia Biotech) at a flow rate of 0.5 ml per min in PBS. Protein concentrations were determined based on absorbance at 280 nM using molar extinction coefficients calculated by the method of Gill and von Hippel (Gill and Hippel, 1989). We derived a factor of 1.0 A_{280} is equal to 540 μg/ml for C6.5-Fc and 620 μg/ml for C25-Fc, based on a calculated molecular weight of 106,000 for each.

2.6. Glycosylation analysis

Samples of the scFv-Fc fusions were de-glycosylated using PNGase F (New England Biolabs, Beverley, MA) under denaturing according to the manufacturer's instructions and analyzed by SDS–PAGE followed by silver staining (Biorad Silver Stain Plus).

2.7. Cytotoxicity assay

Procedures were performed in round-bottom microtiter plates (Costar) using a lactate dehydrogenase (LDH) detection kit (Boehringer Manheim). Briefly, 10,000 HER2/*neu* expressing target cells (SKBR-3) in 50 μl of complete media/well were co-cultured with various numbers of effector peripheral blood mononuclear cells (PBMC) added in 100 μl medium/well. Different concentrations of C6.5-Fc fusion protein antibody were added to appropriate cultures in 50 μl volumes (final volume per well, 200 μl). Cultures were performed in triplicates and plates were incubated for 4 h, after which time the plates were centrifuged and 100 μl supernatant were carefully removed from each well and transferred to corresponding wells of a flat bottom microtiter plate. To determine the LDH activity, 100 μl reaction mixture (cytotoxicity kit) are added to each well and the plates were further incubated for 30 min at room temperature for color development. The amount of LDH activity released and detected colorimetrically in the culture supernatant correlates to the proportion of lysed cells. The absorbance of the supernatants is measured at 490 nm and the data are expressed as mean absorbance. The percent cytotoxicity was calculated as follows: percent cytotoxicity $=[(A-B)/(C-B)]\times 100$ where A = the mean absorbance of supernatants from test cultures; B = the mean absorbance of supernatants from cultures containing target cells only (spontaneous LDH release); and C = the mean absorbance of supernatants from cultures containing target cells cultured in the presence of 2% Triton (maximum LDH release). The data were adjusted in accordance with absorbance of supernatants from cultures of PBMC plus C6.5-Fc fusion protein as well as the absorbance of medium devoid of any cells.

2.8. Equilibrium constant (K_d) determination

Affinity measurements were performed on a Kinexa instrument from Sapidyne Instruments, Boise, ID. PMMA beads (Sapidyne Instruments) were coated with antigen (either recombinant BotNT/A Hc fragment or HER2/*neu* extracellular domain) at 50 μg/ml in PBS overnight at 4°C. The beads were washed three times with PBS and blocked with 0.2 μm filtered 2% skimmed milk powder in PBS (MPBS) for 30 min. scFv-Fc fusions were incubated with dilutions of antigen for 4 h in MPBS. The concentration of the C6.5-Fc fusion in the reaction was 10 nM and 1 nM for the C25-Fc fusion. The amount of uncomplexed antibody in the equilibrium reaction was quantified by capture on the antigen coated PMMA beads, followed by detection with 1:1000 dilution of Cy5 labeled goat anti-human Fc antibody (Jackson Laboratories). Reactions were run in duplicate and fluorescent signals were plotted

as function of antigen concentration. Equilibrium constants were determined using the software provided by the manufacturer (Sapidyne Instruments). The Kinexa assay has been described in detail (Blake et al., 1997).

2.9. Radiolabeling

The C6.5-Fc was labeled with iodine-125 using iodobeads (# 28665X, Pierce; Rockford IL) according to the methods described by the manufacturer. Briefly, 0.5 mg of C6.5-Fc in 250 ml 0.1 M phosphate buffer (pH 6.5) were combined with 0.5 mCi (1.25 ml) of iodine-125 (#NEZ033H, DuPont NEN, Wilmington, DE), and one iodobead. The mixture was incubated for 3 min at room temperature. Unincorporated radioiodine was separated from the labeled protein by gel filtration using the G-50-80 centrifuged-column method (Meares et al., 1984). The immunoreactivity of the C6.5-Fc was evaluated in a live cell binding assay utilizing HER2/*neu* expressing SK-OV-3 cells (Adams et al., 1993). Ten nanograms of labeled C6.5-Fc in 100 ml PBS was added in triplicate to 5×106 SK-OV-3 cells in 15 ml polypropylene centrifuge tubes. After a 30 min incubation at room temperature the cells were washed with 2.0 ml of PBS and centrifuged for 5 min at 500×*g*. Supernatants were separated from the cell pellets, both were transferred to 12×75 counting tubes, counted in a gamma well counter (Gamma 4000, Beckman Instruments, Irvine, CA) and the percentage of activity associated with the cell pellet was determined. Fifty three percent of the activity was found to be associated with the cell pellet. While the maximum possible value in this assay is about 80%, the degree of retention is dictated by a number of factors including the affinity of the molecule for the target antigen. These results are within the normal range observed for radioiodinated C6.5 scFv, indicating to us that the C6.5-Fc was still reactive with cell surface HER2/*neu*.

2.10. Pharmacokinetics

Four-month-old inbred male C.B17/Icr-*scid* (scid) mice were obtained from the Fox Chase Cancer Center Laboratory Animal Facility. Lugol's solution was placed in the drinking water to block thyroid accumulation of radioiodine. Two days later, pharmacokinetic studies were initiated. Twenty micrograms of ^{125}I-C6.5-Fc were administered to three cohorts of four mice by i.v. tail vein injection and to three cohorts of four mice by i.p. injection. Total injected doses were determined by counting each animal on a Series 30 multichannel analyzer/probe system (probe model #2007, Canaberra, Meridian, CT). Blood samples (20-75 μl) were obtained by retro-orbital bleeds from all mice at 5 min post injection and then from alternating groups at subsequent time points (e.g., group I at 15 min, group II at 30 min, group III at 1 h, etc.). The blood samples were counted along with standards in a gamma counter (Beckman, 4000) and the percent of the injected dose retained per ml (% ID/ml) of blood over time was determined for each mouse. The mean values were determined for each time point and the pharmacokinetics were determined using the NCOMP program (Laub and Gallo, 1996).

3. Results

3.1. Plasmid constructions

We have constructed a plasmid for the expression of single-chain antibody Fv domains (scFv) fused to the human IgG1 Fc domain to make a bivalent, ~106,000 molecular weight scFv-Fc fusion (Fig. 1). Plasmid pPIgG1 for the expression of the scFv-Fc fusions (comprising the scFv followed by the hinge, C_H2 and C_H3 domains of human IgG1) is based on the *Pichia pastoris* expression plasmid pPICZαA (Invitrogen). This plasmid uses the alcohol oxidase (AOX1) promoter for high level expression of heterologous proteins, which are secreted to the media under direction of the *Saccharomyces cerevisiae* a-factor signal sequence.

Details of the plasmid and the cloning sites are shown in Fig. 2. The human hinge, C_H2, and C_H3 domains of IgG1 were cloned into the *Not*I and *Xba*I sites of pPICZαA, creating plasmid pPIgG1. A stop codon was included in the construct following the final amino acid of the C_H3 domain; therefore the myc epitope tag and $(His)_6$ sequences from pPICzαA are not expressed in the fusion protein.

scFv genes to be expressed as scFv-Fc fusions in pPIgG1 are amplified by PCR and subcloned into pPIgG1 using the 5′ *Xho*I site in the alpha factor

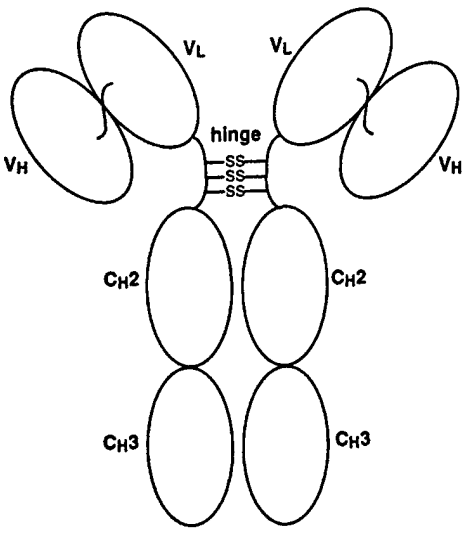

Fig. 1. Schematic representation of a dimeric scFv-Fc fusion. V_H, heavy chain variable domain; V_L, light chain variable domain: C_H2 and C_H3, heavy chain constant domains 2 and 3; –SS– indicates disulfide bonds between the hinge domains.

signal sequence and the 3′ *Not*I site which sits just before the beginning of the IgG hinge (Fig. 2). The 5′ PCR primer, in addition to appending an *Xho*I site, must also be designed to recreate the amino acid sequence of the alpha amylase signal from the *Xho*I site to the end of the signal peptide, positioning the 5′ end of the scFv flush with the end of the signal. The 3′ PCR primer can be either a sequence-specific primer which appends a *Not*I site onto the end of the scFv gene, or a universal downstream primer for amplifying from vectors such as the phage display vector pHEN1 which already has an in-frame *Not*I site positioned at the end of the scFv gene (Hoogenboom et al., 1991). We subcloned two model scFvs into the pPIgG1 vector for evaluation: C25, which recognizes the botulinum neurotoxin serotype A binding domain (BotNT/A Hc) (Amersdorfer et al., 1997), and C6.5, which recognizes the HER2/*neu* protein (Schier et al., 1995). The constructs were electroporated into *Pichia pastoris* strain GS115 for expression.

3.2. Small scale expression and screening of Pichia transformants

Since protein expression levels in *Pichia* from integrated pPICZα-derived plasmids can vary depending on site of integration and copy number, we

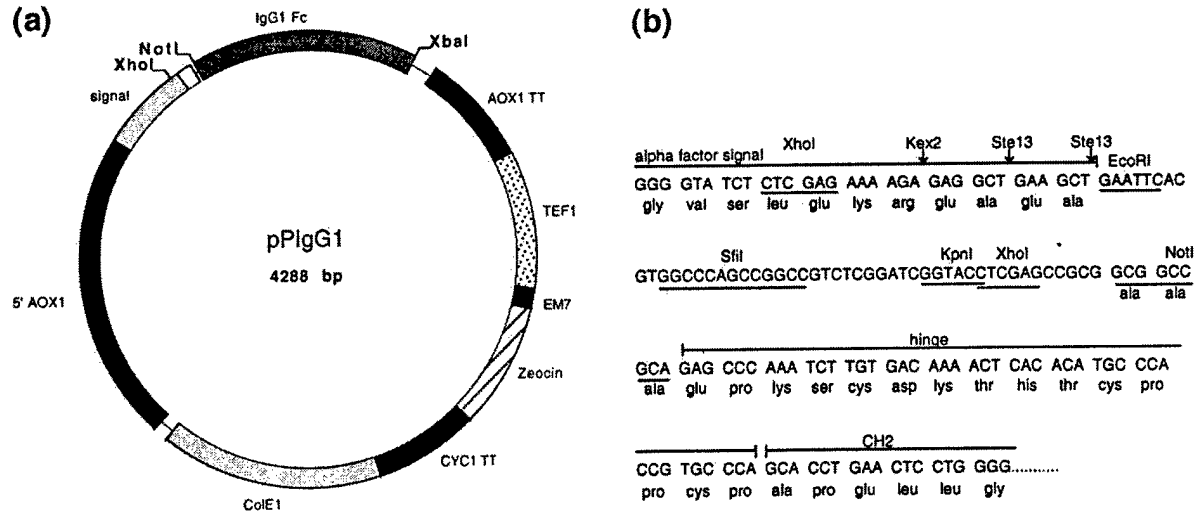

Fig. 2. (A) Schematic of plasmid pPIgG1. 5′ AOX1, alcohol oxidase 1 promoter; AOX1 TT, transcriptional terminator from *Pichia pastoris* AOX1 gene; TEF1 promoter, transcriptional elongation factor 1 promoter from *Saccharomyces cerevisiae*; EM7 promoter, synthetic prokaryotic promoter; Zeocin, Zeocin resistance gene; CYC1 TT, transcriptional terminator from *Saccharomyces cerevisiae* CYC1 gene; ColE1, ColE1 origin of replication. (B) Details of the cloning sites of pPIgG1. Restriction endonuclease sites are underlined, arrows indicate cleavage sites within the alpha mating factor signal sequence for Kex2 and Ste13 proteases.

screened multiple transformants for scFv-Fc expression levels. Four clones apiece of the pPIgG1-C25 and pPIgG1-C6.5 Zeocin-resistant transformants (along with pPICZαA as a control) were grown and induced in 10 ml of BMMY media at 30°C for 72 h as described in Materials and methods. Cultures supernatants were analyzed on SDS–PAGE under reducing conditions followed by silver stain detection. Results show that a new band appears in the media with an apparent molecular weight of ~55,000 daltons, in good agreement with the predicted 53,000 dalton molecular weight of a reduced scFv-Fc fusion (Fig. 3 panel A). Close inspection shows that this band is actually a closely spaced doublet of bands with similar mobilities. Western blotting analysis demonstrates that these bands react with an anti-human Fc specific antibody (Fig. 3 panel B). No anti-Fc reactive species were seen in *Pichia* GS115 cells transfected with the control plasmid (pPICZαA). On non-reducing SDS–PAGE gels, the scFv-Fc protein bands have approximately twice the apparent molecular weight, indicating that the scFv-Fc fusions are secreted to the media primarily as disulfide-linked dimers (not shown). Expression levels of the C6.5-Fc clones are somewhat less than that of the C25-Fc clones. Two well-expressing clones were chosen for large scale expression and analysis.

3.3. Large scale expression and purification of scFv-Fc fusions

One liter of culture media was used to generate pure C25-Fc and C6.5-Fc fusions for characterization. Briefly, the purification employed was ammonium sulfate precipitation of the proteins from the culture supernatants, followed by dialysis, Protein G affinity chromatography, and gel filtration chroma-

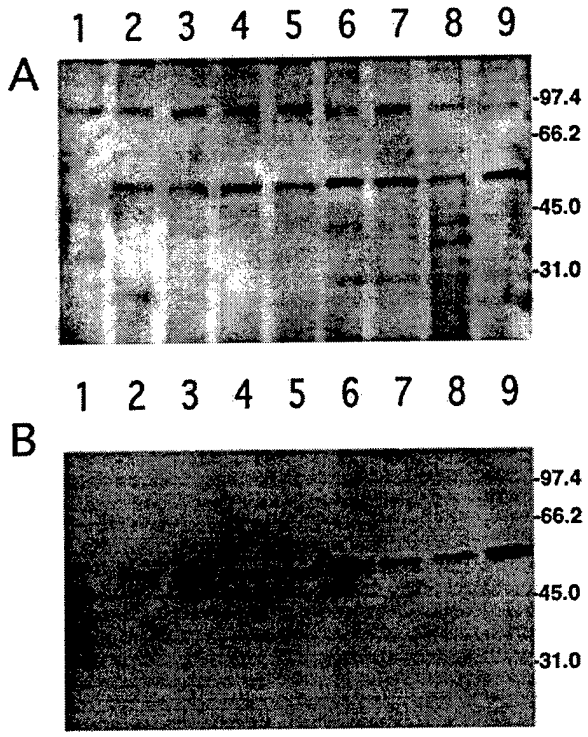

Fig. 3. Analysis of scFv-Fc expression in *Pichia pastoris* strain GS115. (A) Silver stained SDS–PAGE gel of culture supernatants. Lane 1, pPICZαA control transformant; lanes 2-5, pPIgG1-C6.5 transformants; lanes 6-9, pPIgG1-C25 transformants. (B) Western blot of a duplicate of the above gel using anti-human IgG (Fc-specific)-HRP (horse radish peroxidase) conjugate, followed by ECL development. Molecular weight markers (kDa) are indicated on right of each gel.

tography. Fig. 4, panel A shows fractions from a typical purification. After ammonium sulfate precipitation, the ~55 kDa scFv-Fc fusion protein doublet is clearly visible (lanes 1 and 4). After Protein G affinity chromatography (lanes 2 and 5) the scFv-Fc fusion protein is substantially pure, with a number of smaller bands copurifying which may represent breakdown products which also bind to Protein G. These lower molecular weight species are removed by gel filtration on Superdex S-200 (Amersham Pharmacia Biotech) (lanes 3 and 6). The yield after purification was ~2 mg/l of culture for C25-Fc and ~300 μg/l of culture for the C6.5-Fc fusion. The purified scFv-Fc fusion protein is a disulfide-linked dimer, as shown by SDS–PAGE analysis under reducing and non-reducing conditions (Fig. 4B). The dimeric nature of the scFv-Fc was also confirmed by molecular weight analysis on Superdex S-200 gel filtration vs. molecular weight standards (not shown).

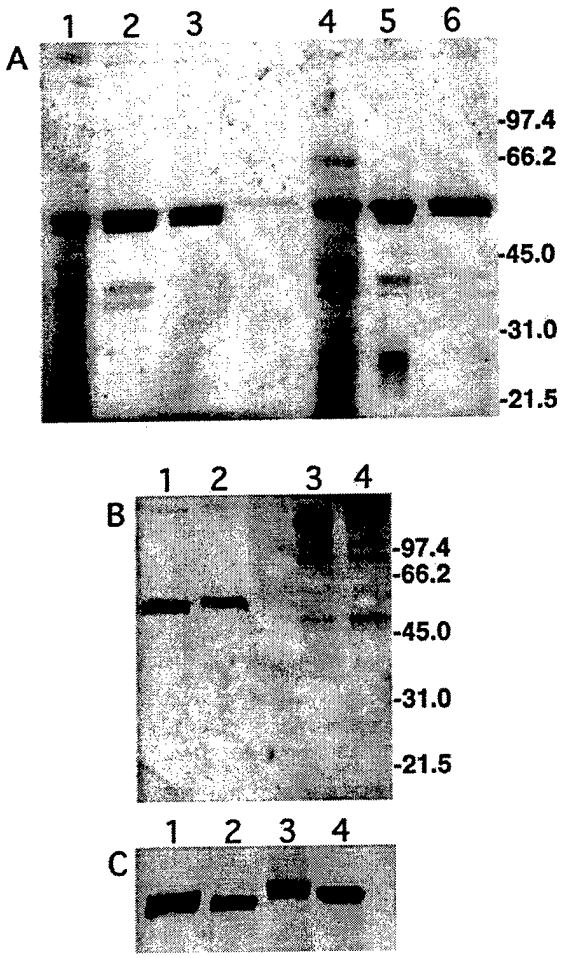

Fig. 4. (A) SDS–PAGE analysis of samples from representative purifications of the C6.5 and C25-Fc fusion proteins. Lane 1, ammonium sulfate pellet of C6.5-Fc; lane 2, protein G pool of C6.5-Fc; lane 3, S200 pool of C6.5-Fc; lane 4, ammonium sulfate pellet of C25-Fc; lane 5, protein G pool of C25-Fc; lane 6, S200 pool of C25-Fc. (B)SDS–PAGE analysis of the purified scFv-Fc fusions under reducing and non-reducing conditions. Lanes 1 and 3, purified C6.5-Fc, lanes 2 and 4, purified C25-Fc protein. Lanes 1 and 2 are under reducing conditions, lanes 3 and 4 under non-reducing conditions. Molecular weight standards (kDa) are to the right. (C) PNGase F analysis of glycosylation of the C6.5-Fc and C25-Fc fusions. Lane 1 and 2, C6.5-Fc; lanes 3 and 4, C25-Fc. Lanes 1 and 3 are minus PNGase F; lanes 2 and 4 are plus PNGase F.

The final purified scFv-Fc proteins migrate in reducing SDS–PAGE as a tight doublet of bands with an apparent molecular weight of ~55,000 daltons. The molecular weight heterogeneity observed could be due to differences in glycosylation, or in the processing of the alpha amylase signal peptide. To explore these possibilities, the purified fusions were subjected to N-terminal sequencing and de-glycosylation analysis with PNGase F.

N-terminal analysis results indicated that both the upper and lower bands of the doublet, for both C6.5-Fc and C25-Fc proteins, begin with the amino acid sequence glu-ala-glu-ala..., indicating that signal peptide cleavage had occurred after the Kex2 site in the alpha amylase leader, but that Ste13 cleavage had not occurred (Fig. 2). The samples were further analyzed by deglycosylation with PNGase F (Fig. 4C). After deglycosylation of both the fusion proteins, the doublet collapsed to a single band, indicating that the observed heterogeneity is due to N-linked glycosylation of the higher molecular band and no glycosylation of the lower molecular weight band.

3.4. Affinity (K_d) analysis

We wished to show that the scFv antigen binding site in the scFv-Fc fusion retained the affinity of the unfused scFv. The affinities of our model scFvs for their antigens have been previously determined by kinetic analysis of association and dissociation rate constants (k_{on} and k_{off}) by surface plasmon resonance (Amersdorfer et al., 1997; Schier et al., 1995);

from the k_{on} and k_{off} values the equilibrium dissociation constants (K_ds) of C6.5 and C25 were calculated to be 16 nM and 1 nM, respectively. We determined equilibrium dissociation constants under equilibrium conditions using a Kinexa instrument (Sapidine Instruments) (Blake et al., 1997). We determined the K_ds of the C6.5-Fc and C25-Fc fusion proteins to be 4.6 nM and 0.5 nM, respectively, for their cognate antigens. While the different experimental techniques do not allow a direct comparison of the K_d values, and we cannot rule out subtle differences in affinity between the scFv and scFv-Fc fusion formats, it is clear that the scFv binding sites retain high affinity for their cognate antigens in the scFv-Fc fusion format.

3.5. ADCC assays

The C6.5-Fc fusion protein was assayed to determine if the Fc domain of the fusion was functionally able to direct antibody-dependent cell cytotoxicity (ADCC) towards antigen expressing target cells. 10,000 HER2/*neu* expressing SKBR3 target cells were co-cultured with effector PBMC (peripheral blood mononuclear cells) at 100:1, 50:1, and 25:1 ratios in the presence of various concentrations of C6.5-Fc. After 4 h incubation, the samples were analyzed for percent cell lysis by lactate dehydrogenase (LDH) release. Results (Fig. 5) show PBMC killing of target cells occurs in a dose dependent fashion with C6.5-Fc.

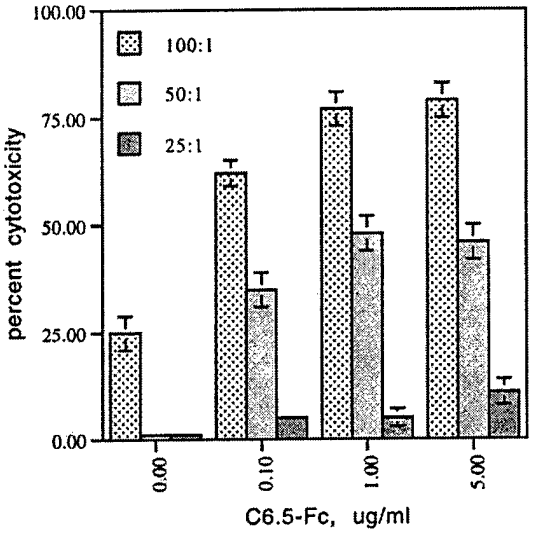

Fig. 5. ADCC (antibody-dependent cellular cytotoxicity) assays of the C6.5-Fc fusion protein using PBMC effector cells and HER2/*neu* expressing SKBR3 cells as target. Shaded bars indicates different effector cell: target cell ratios.

3.6. Pharmacokinetics

Single-chain Fv antibodies are rapidly cleared from the bloodstream in mouse models, with typical $t_{1/2}$ of the beta clearance of approximately 3.5 h (Huston et al., 1996). Similarly, in previous studies of C6.5 scFv pharmacokinetics in scid mice, a $t_{1/2}$ β of 3.0 h was determined (G. Adams, unpublished data). This rapid clearance prevents the characterization of scFv in animal models for efficacy where a longer serum half-life is required to observe a biological effect. We wished to determine if the fusion of a model single-chain antibody Fv domain to a Fc domain would impart a longer serum half life to the scFv. C6.5-Fc was labeled with iodine-125 using iodobeads, evaluated in a live cell binding assay utilizing HER2/*neu* expressing SK-OV-3 cells for retention of activity. (Adams et al., 1993), and administered to four month old inbred male C.B17/Icr-*scid* (scid) mice as described in Materials and methods. Both intravenous (tail vein) and intraperitoneal routes of administration were studied. Results are shown in Fig. 6. After a rapid tissue distribution (alpha phase), the scFv-Fc fusion is cleared in the beta phase of elimination more slowly, with the $t_{1/2}$ β of 37.3 h for intravenous and 92.8 h for intraperitoneal injections. This represents a more than 12-fold and more than 30-fold improvement over the 3.0 h $t_{1/2}$ β observed for a C6.5 scFv alone. In contrast to a typical scFv, which is practically undetectable in mouse serum 12 h past injection, the slower clearance of the scFv-Fc fusion results in substantial levels of scFv in the blood at longer times, with approximately 5% of the injected dose still in the serum at 48 h after injection for both i.v. and i.p. injections.

4. Discussion

The single-polypeptide, minimally sized scFv antibody fragment is useful for the design and

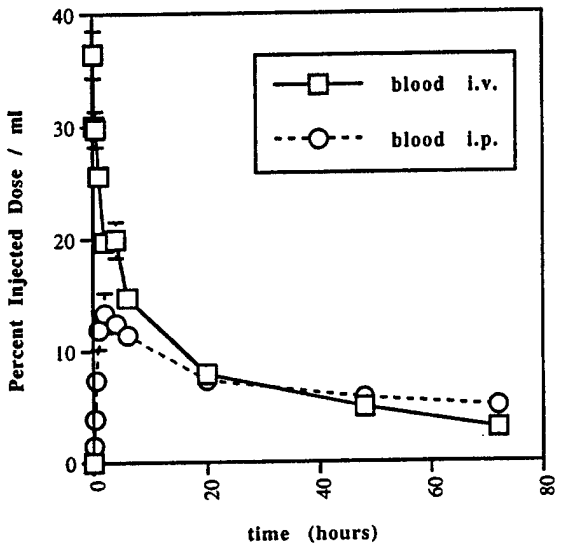

Fig. 6. Kinetics of clearance of C6.5-Fc fusion from mouse serum. Mice received ^{125}I-labeled C6.5-Fc protein by either intravenous or intraperitoneal injection. Each data point represents the mean value for four mice.

construction of phage display antibody libraries, as fusion proteins, and as intrabodies; in addition the small size is best suited to tumor targeting due to superior tissue penetration (Yokata et al., 1992). However useful, the scFv format suffers from a number of key limitations. The lack of avidity due to monovalent binding can limit the effectiveness and/or sensitivity of scFv fragments in many immunochemical applications such as FACS and ELISA. Also, the scFv fragment typically needs to be 'tagged' in some way, such as a hexahistidine or epitope tag, to allow detection and purification. Perhaps most importantly, in vivo characterization of scFv in animal models can be impossible because of their rapid clearance from the bloodstream due to their small size. (Huston et al., 1996)

It would be desirable to be able to easily reengineer a scFv into an IgG-like format that combines the affinity and specificity of the scFv with the bivalency, pharmacokinetics, and effector functions of a complete immunoglobulin. One way is to clone the V_H and V_L genes from the scFv and reclone them into a full-length IgG expressing vector (Persic et al., 1997). However this requires separate cloning steps for the V_H and V_L, and it can require significant amounts of time to make a stable IgG secreting tissue culture line.

As an alternative, we have constructed a vector, pPIgG1, to express a scFv-Fc fusion (in which the scFv is fused to the hinge, C_H2, and C_H3 domains of human IgG1) in the yeast *Pichia pastoris* (Fig. 1). The scFv is expressed and secreted as a glycosylated, disulfide-linked dimer at high yields in the culture medium. The scFv-Fc fusion combines the affinity and specificity of the scFv antigen binding site with Fc-mediated dimerization. In addition, the Fc domain is a convenient affinity 'handle' for the purification and detection of the scFv species by reagents like protein A, protein G, and anti-Fc antibodies (Figs. 3B and 4A). An additional major advantage of *Pichia pastoris* over mammalian cell culture production is that *Pichia* can be readily fermented to high OD and high protein expression levels (Cregg and Higgins, 1995). This construct is similar to scFv-Fc fusions that other workers have made in mammalian and insect cells (Brocks et al., 1997; Hayden et al., 1994; Kato et al., 1995; Ma et al., 1996; Shu et al., 1993), however this is the first time to our knowledge that such a fusion has been expressed in yeast.

We have cloned and expressed two model scFv into pPIgGl for evaluation of our system: C25, which recognizes the botulinum neurotoxin serotype A binding domain (BotNT/A Hc) (Amersdorfer et al., 1997), and C6.5, which recognizes the HER2/*neu* protein (Schier et al., 1995). Yields of the scFv-Fc fusions vary depending on the nature of the scFv, from ~2 mg/l for the best expressor (C25-Fc) to ~300 μg/l for the C6.5-Fc fusion in shaker flasks. By an equilibrium K_d determination, we have shown that the scFv domain of the fusion retains the affinity of the parent scFv for its cognate antigen.

The use of scFv antibody fragments in FACS can be limited due to monovalent binding and lack of a good detection method. In favorable circumstances, we and other investigators have demonstrated the use of scFv from phage display libraries as FACS reagents, either directly as scFv-phage, or as isolated scFv fragments (de Kruif et al., 1995). However, we have found that the utility of scFv as FACS reagents must be evaluated on a case-by-case basis. For example, previous studies of C6.5 scFv protein on HER2/*neu* positive SK-OV-3 cells showed that the

half-life ($t_{1/2}$) of the monovalent C6.5 scFv on the cell surface was much less than 5 min; efficient staining required preparing biotinylated scFv, staining the cells with biotinylated scFv, fixing the stained cells in paraformaldehyde, and detection with PE labeled streptavidin (Schier et al., 1996). In contrast, we routinely use the C6.5-Fc fusion protein in FACS assays on HER2/*neu* expressing cells without any modification of the protein or fixing of the target cells; detection is accomplished with fluorescently labeled anti-Fc antibodies (M.A. Poul, not shown). In addition, superior binding of a bivalent scFv-Fc to a cell surface antigen due to avidity also results in superior sensitivity over a monovalent scFv. This could be of obvious benefit for use of phage display library derived scFv to study cell surface expression of target molecules, especially where low levels of cell surface antigen need to be detected.

For in vivo characterization of scFv species, a long serum half-life will be needed in many instances to observe a biological effect. Previous experiments in mice have shown that the $t_{1/2}$ for the beta phase of elimination for scFvs are typically 3.5 h (Huston et al., 1996). Similarly, in previous studies of C6.5 scFv pharmacokinetics in scid mice, a $t_{1/2}$ β of 3.0 h was determined (G. Adams, unpublished data). We have shown in these experiment a significant increase of the $t_{1/2}$ β of the C6.5-Fc fusion to 37.3 and 92.8 h for intravenous and intraperitoneal injections, respectively. This represents greater than 12-fold and 30-fold improvements in the half life, resulting in significant serum levels (~5% of the injected dose/ml) even at 48 h post injection. We have recently used the superior pharmacokinetics of pPIgG1 derived scFv-Fc fusions to demonstrate in vivo Botulinum toxin neutralization with scFv selected from phage display libraries (Amersdorfer, Powers, and Marks, manuscript in preparation).

In contrast to a typical immunoglobulin, pharmacokinetic analysis of the C6.5-Fc fusion when administered by i.v. injection shows a significant and rapid clearance of ~80% of the fusion protein in the alpha phase (Fig. 6). We speculate that this may be due to the nature of carbohydrate attached to the *Pichia* derived scFv-Fc fusion. Glycosylation patterns on immunoglobulin species can have profound effects on antibody effector function and pharmacokinetics (reviewed in Wright and Morrison, 1997). Yeast in general attach high-molecular weight mannose structures (Jahn-Schmid et al., 1996), although in *Pichia pastoris* these residues are generally shorter than in *Saccharomyces cerevisiae* (Cregg and Higgins, 1995). Terminally mannosylated carbohydrates on immunoglobulins can be rapidly cleared by binding to high-affinity mannose receptors in the liver; this clearance can be partially prevented by co-injection of mannan (Wright and Morrison, 1994). Since complete deglycosylation of an IgG results in normal antigen affinity while retaining some (but not all) effector functions (Leatherbarrow et al., 1985; Tao and Morrison, 1989; Walker et al., 1989; Wright and Morrison, 1997), it may be possible to further improve the pharmacokinetics of the *Pichia* derived scFv-Fc fusions by eliminating the N-linked glycosylation site from the Fc domain by site-directed mutagenesis.

We have recently modified the pPIgG1 vector to further increase its utility. At present cloning into pPIgG1 requires using the 5′ *Xho*I site in the alpha factor signal sequence and reconstruction by the PCR primer of the last few amino acids in the signal sequence. Since N-terminal sequence analysis shows that the final four amino acids of the signal (glu-ala-glu-ala . . .) are not cleaved from the C6.5-Fc and C25-Fc fusions, we have mutated the alpha factor signal sequence to end in glu-ala-*met*-ala . . . , and incorporated a *Nco*I site (CCATGG) around the minus 2 position methionine codon (ATG). In addition a second *Nco*I site in the pPICZαA vector was eliminated by site-directed mutagenesis. This modified vector (pPIgG2) allows scFv to be removed and subcloned by a simple *Nco*I-*Not*I digest from our preferred scFv phage display vector pHEN1 (Hoogenboom et al., 1991) (D. Powers, unpublished results).

As more and more scFv from phage display libraries are developed for research, diagnostic, and therapeutic uses, it will be increasingly more important to have simple, rapid techniques to reengineer the scFv into appropriate formats for characterization. The *Pichia pastoris* scFv-Fc fusion protein system allows a simple, rapid way to combine the affinity and specificity of a scFv with the Fc mediated bivalency, prolonged serum half life, and effector functions of an IgG.

Acknowledgements

We would like to thank Mr. Tom Purcell of Invitrogen Co. for helpful discussions, Mr. Steve Chen for technical assistance, and Dr. Chris Turk of UCSF for N-terminal sequence analysis. This work was partially funded by DAMD17-94-C-4034, DAMD17-94-J-4433, and NIH CA65559.

References

Adams, G.P., McCartney, J.E., Tai, M.-S. et al., 1993. Highly specific in vivo tumor targeting by monovalent and divalent forms of 741F8 anti-c-erbB-2 single chain Fv. Cancer Res. 53, 4026.

Adams, G.P., McCartney, J.E., Wolf, E.J. et al., 1995. Enhanced tumor specificity with stably iodinated 741F8-2 (sFv')2, an anti-c-erbB-2 single chain Fv dimer. J. Nucl. Med. 36, 2276.

Adams, G.P., Schier, R., Marshall, K. et al., 1998. Increased affinity leads to improved selective tumor delivery of single-chain Fv antibodies. Cancer Res. 58, 485.

Amersdorfer, P., Wong, C., Chen, C. et al., 1997. Molecular characterization of murine humoral immune response to botulinum neurotoxin type A binding domain as assessed by using phage antibody libraries. Infect. Immun. 65, 3743.

Bird, R.E., Hardman, K.D., Jacobson, J.W. et al., 1988. Single-chain antigen-binding proteins. Science 242, 423.

Blake, D.A., Khosraviani, M., Pavlov, A.R., Blake, R.C., 1997. Characterization of a metal-specific monoclonal antibody. Immunochem. Technol. Environ. Applic. 657, 49.

Brocks, B., Rode, H.J., Klein, M. et al., 1997. A TNF receptor antagonistic scFv, which is not secreted in mammalian cells, is expressed as a soluble mono- and bivalent scFv derivative in insect cells. Immunotechnology 3, 173.

Chamow, S., Ashkenazi, M.A., 1999. Antibody Fusion Proteins. John Wiley, New York.

Cregg, J.M., Higgins, D.R., 1995. Production of foreign proteins in the yeast *Pichia pastoris*. Canadian J. Botany 73, S891.

de Kruif, J., Terstappen, L., Boel, E., Logtenberg, T., 1995. Rapid selection of cell subpopulation-specific human monoclonal antibodies from a synthetic phage antibody library. Immunology 92, 3938.

Gill, S.C., Hippel, P.H.V., 1989. Calculation of protein extinction coefficients from amino acid sequence data. Anal. Biochem. 182, 319.

Hayden, M.S., Linsley, P.S., Gayle, M.A. et al., 1994. Single-chain mono- and bispecific antibody derivatives with novel biological properties and antitumor activity from a COS cell transient expression system. Ther. Immunol. 1, 3.

Hoogenboom, H.R., 1997. Mix and match: building manifold binding sites. Nature Biotechnol. 15, 125.

Hoogenboom, H.R., Griffiths, A.D., Johnson, K.S. et al., 1991. Multi-subunit proteins on the surface of filamentous phage: methods for displaying antibody (Fab) heavy and light chains. Nucleic Acids Res. 19, 4133.

Huston, J.S., George, A.J.T., Adams, G.P. et al., 1996. Single-chain Fv radioimmunotargeting. Q. J. Nucl. Med. 40, 320.

Huston, J.S., Levinson, D., Mudgett-Hunter, M. et al., 1988. Protein engineering of antibody binding sites: recovery of specific activity in an anti-digoxin single-chain Fv analogue produced in Escherichia coli. Proc. Natl. Acad. Sci. USA 85, 5879.

Jahn-Schmid, B., Graninger, M., Glozik, M. et al., 1996. Immunoreactivity of allergen (Bet v 1) conjugated to crystalline bacterial cell surface layers (S-layers). Immunotechnology 2, 103.

Kato, T., Sato, K., Suzuki, S. et al., 1995. Mammalian expression of single chain variable fragments dimerized by Fc regions. Mol. Biol. Rep. 21, 141.

Laub, P.B., Gallo, J.M., 1996. NCOMP, a Windows-based computer program for noncompartmental analysis of pharmacokinetic data. J. Pharm. Sci. 85, 393.

Leatherbarrow, R.J., Rademacher, T.W., Dwek, R.A. et al., 1985. Effector functions of a monoclonal aglycosylated mouse IgG2a: binding and activation of complement component C1 and interaction with human monocyte Fc receptor. Mol. Immunol. 22, 407.

Ma, S., Thompson, J., Hu, H., Neville, D.M., 1996. Expression and characterization of a divalent chimeric anti-human CD3 single-chain antibody. Scand. J. Immunol. 43, 134.

Marasco, W.A., 1997. Intrabodies: turning the humoral immune system outside in for intracellular immunization. Gene Ther. 4, 11.

Marks, J.D., Hoogenboom, H.R., Bonnert, T.P., McCafferty, J., Griffiths, A.D., Winter, G., 1991. By-passing immunization: human antibodies from V-gene libraries displayed on phage. J. Mol. Biol. 222, 581.

McCafferty, J., Griffiths, A.D., Winter, G., Chiswell, D.J., 1990. Phage antibodies: filamentous phage displaying antibody variable domains. Nature 348, 552.

Meares, C.F., McCall, M.J., Reardan, D.T., Goodwin, D.A., Diamanti, P.I., McTigue, M., 1984. Conjunction of antibodies with bifunctional chelating agents: isothiocyanate and bromoacetamide reagents, methods of analysis, and subsequent addition of metal ions. Anal. Biochem. 142, 68.

Persic, L., Roberts, A., Wilton, J., Cattaneo, A., Bradbury, A., Hoogenboom, H.R., 1997. An integrated vector system for the eukaryotic expression of antibodies and their fragments after selection from phage display libraries. Gene 187, 9.

Poul, M.-A., Cerutti, M., Chaabihi, H., Devauchelle, G., Kaczorek, M., Lefranc, M.-P., 1995. Design of cassette baculovirus vectors for the production of therapeutic antibodies in insect cells. Immunotechnology 1, 189.

Schier, R., Marks, J.D., Wolf, E.J. et al., 1995. In vitro and in vivo characterization of a human anti-c-erbB-2 single-chain Fv isolated from a filamentous phage antibody library. Immunotechnology 1, 73.

Schier, R., McCall, A., Adams, G.P. et al., 1996. Isolation of picomolar affinity anti-c-erbB-2 single-chain Fv by molecular evolution of the complementarity determining regions in the center of the antibody binding site. J. Mol. Biol. 263, 551.

Shu, L., Qi, C.F., Schlom, J., Kashmiri, S.V., 1993. Secretion of a single-gene-encoded immunoglobulin from myeloma cells. Proc. Natl. Acad. Sci. USA 90, 7995.

Tao, M.-H., Morrison, S.L., 1989. Studies of aglycosylated chimeric mouse-human IgG. Role of carbohydrate in the structure and effector functions mediated by the human IgG constant region. J. Immunol. 143, 2595.

Walker, M.R., Lund, J., Thompson, K.M., Jefferis, R., 1989. Aglycosylation of human IgG1 and IgG3 monoclonal antibodies can eliminate recognition by human cells expressing Fc gamma RI and/or Fc gamma RII receptors. Biochem. J. 259, 347.

Wright, A., Morrison, S.L., 1994. Effect of altered CH2-associated carbohydrate structure on the functional properties and in vivo fate of chimeric mouse-human immunoglobulin G1. J. Exp. Med 180, 1087.

Wright, A., Morrison, S.L., 1997. Effect of glycosylation on antibody function: implications for genetic engineering. Trends Biotechnol. 15, 26.

Yokata, T., Milenic, D.E., Whitlow, M., Schlom, J., 1992. Rapid tumor penetration of a single-chain Fv and comparison with other immunoglobulin forms. Cancer Res. 52, 3402.

#1840 TARGETING OF BIVALENT ANTI-HER2/NEU DIABODY ANTIBODY FRAGMENTS TO TUMOR CELLS IS INDEPENDENT OF THE INTRINSIC ANTIBODY AFFINITY. Ulrik B Nielsen, Gregory P Adams, Louis M Weiner, and James D Marks, *Dept of Anesthesia and Pharm Chem, UCSF, San Francisco, CA, and Dept of Med Oncology, Fox Chase Cancer Ctr, Philadelphia, PA*

Single-chain Fv molecules penetrate tumors rapidly, have fast serum clearance, and excellent tumor to normal organ ratios. However, due to the rapid serum clearance and monovalent nature of the scFv, only small quantities are retained within the tumor. To study the effect of an additional binding site on tumor targeting, bivalent diabody molecules were constructed from three affinity mutants of the human anti-HER2/neu (c-ErbB2) scFv molecule C6.5. The affinity of the parental scFv's vary 133 fold from 133 nM (C6G98A), 25 nM (C6.5), to 1 nM (C6ML3-9), but differ by only 1-3 amino acids and recognize the same epitope. Binding kinetics was determined by surface plasmon resonance (SPR) on immobilized c-ErbB2 extracellular domain. Association constants obtained for diabody molecules were similar to those of the parental scFv. Dissociation rates decreased with prolonged association time. After 2 hrs of association, the decrease in the bivalent dissociation constant was inversely proportional to that of the monovalent interaction, ranging from only 2-fold for that of the C6ML3-9 diabody to 17-fold for the C6G98A diabody. Biodistribution studies were performed in SCID mice bearing established SKOV-3 tumors. At 24 hrs, 3 to 37 fold more diabody was retained in tumor compared to the parental scFv. This likely results from a higher apparent affinity, due to bivalent binding, and a slower serum clearance. Surprisingly, the difference in affinity between diabodies did not significantly alter the quantitative tumor retention or specificity of the tumor localization. Thus above a threshold affinity, the pharmacokinetics of the antibody fragment is the most important determinant of quantitative tumor delivery.